THE JOURNAL OF COMPARATIVE NEUROLOGY 483:351–373 (2005)

Vglut2 Afferents to the Medial Prefrontal and Primary Somatosensory Cortices: A Combined Retrograde Tracing In Situ Hybridization

ELIZABETH E. HUR AND LASZLO ZABORSZKY*
Center for Molecular and Behavioral Neuroscience, Rutgers, The State University of New Jersey, Newark, New Jersey 07102

ABSTRACT

Glutamate transmission is critical for controlling cortical activity, but the specific contribution of the different isoforms of vesicular glutamate transporters in subcortical pathways to the neocortex is largely unknown. To determine the distribution and neocortical projections of vesicular glutamate transporter2 (Vglut2)-containing neurons, we used in situ hybridization and injections of the retrograde tracer Fluoro-Gold into the medial prefrontal and primary somatosensory cortices. The thalamus contains the majority of Vglut2 cells projecting to the neocortex (~90% for the medial prefrontal cortex and 96% for the primary somatosensory cortex) followed by the hypothalamus and basal forebrain, the claustrum, and the brainstem. There are significantly more Vglut2 neurons projecting to the medial prefrontal cortex than to the primary somatosensory cortex. The medial prefrontal cortex also receives a higher percentage of Vglut2 projection from the hypothalamus than the primary somatosensory cortex. About 50% of thalamic Vglut2 projection to the medial prefrontal cortex and as much as 80% of the thalamic projection to primary somatosensory cortex originate in various relay thalamic nuclei. The remainder arise from different midline and intralaminar nuclei traditionally thought to provide nonspecific or diffuse projection to the cortex. The extrathalamic Vglut2 corticopetal projections, together with the thalamic intralaminar-midline Vglut2 corticopetal projections, may participate in diffuse activation of the neocortex. J. Comp. Neurol. 483:351–373, 2005.

Indexing terms: retrograde transport; basal forebrain; hypothalamus; corticopetal; glutamate

Vesicular glutamate transporters (Vgluts) accumulate glutamate into the synaptic vesicles of excitatory neurons and three isoforms of Vgluts were recently cloned and identified. Vgluts are definitive markers for neurons that use glutamate as neurotransmitter (Ni et al., 1994; Bellocchio et al., 1998, 2000; Aihara et al., 2000; Takamori et al., 2000, 2002; Bai et al., 2001; Fremeau et al., 2001; Fujiyama et al., 2001; Gras et al., 2002; Schafer et al., 2002). Vglut1 and Vglut2 share a complementary distribution, such that Vglut1 is predominantly expressed in the neocortex, whereas Vglut2 mRNA is abundant in subcortical forebrain regions, including thalamic nuclei, hypothalamic areas, basal forebrain, and some amygdaloid nuclei (Fremeau et al., 2001; Herzog et al., 2001; Varoqui et al., 2001). However, both Vglut1 and Vglut2 are codistributed in certain brain regions, such as the hypothalamus (Ziegler et al., 2002; Lin et al., 2003), the medulla oblongata (Stornetta et al., 2002), and cerebellum (Hisano et al., 2002; Hioki et al., 2003). Coexpression of Vglut1 and Vglut2 has also been documented in early development (Fremeau et al., 2004; Wojcik et al., 2004) and in specific regions of the central nervous system such as the trigeminal ganglion neurons (Li et al., 2003). A third unique form (Vglut3) has been found in a subset of neurons in the neocortex, hippocampus, caudate-putamen, dopaminergic midbrain, and the serotoninergic raphe nuclei (Gras et al.,

Grant sponsor: US Public Health Service; Grant number: NS23945 (to L.Z.).

*Correspondence to: Laszlo Zaborszky, Rutgers The State University of New Jersey, 197 University Ave., Newark, NJ 07102. E-mail: zaborszky@axon.rutgers.edu

Received 5 July 2004; Revised 20 September 2004; Accepted 22 November 2004

DOI 10.1002/cne.20444

Published online in Wiley InterScience (www.interscience.wiley.com).

Abbreviations

3V	third ventricle
4V	fourth ventricle
7n	facial nerve
AA	anterior amygdaloid area
ac	anterior commissure
Acb	nucleus accumbens
AcbC	nucleus accumbens, core
AcbSh	nucleus accumbens, shell
AD	anterodorsal thalamic nucleus
AHA	anterior hypothalamic area, anterior
AM	anteromedial thalamic nucleus
AOT	bed nucleus of the accessory olfactory tract
APT	anterior pretectal nucleus
Aq	aqueduct (Sylvius)
ar	acoustic radiation
Arc	arcuate nucleus
AV	anteroventral thalamic nucleus
BM	basomedial amygdaloid nucleus
BL	basolateral amygdaloid nucleus
BLV	basolateral amygdaloid nucleus, ventral part
BSt	bed nucleus of the stria terminalis
cc	corpus callosum
Ce	central amygdaloid nucleus
ChAT	choline acetyl transferase
CL	centrolateral thalamic nucleus
Cl	claustrum
CLi	caudal linear nucleus of the raphe
CM	centromedial thalamic nucleus
Co	cortical amygdaloid nucleus
cp	cerebral peduncle
CPu	caudate-putamen (striatum)
D3V	third ventricle, dorsal part
DE	dorsal endopiriform nucleus
DLG	dorsal lateral geniculate nucleus
DMH	dorsomedial hypothalamic nucleus
DR	dorsal raphe nucleus
DT	dorsal tegmental nucleus
EP	entopeduncular nucleus
F	nucleus of the fields of Forel
f	fornix
FG	Fluoro-Gold
fi	fimbria of the hippocampus
fr	fasciculus retroflexus
FStr	fundus striati
GABA	gamma-aminobutyric acid
GP	globus pallidus
HDB	horizontal limb of the diagonal band of Broca
IAD	interanterodorsal thalamic nucleus
IAM	interanteromedial thalamic nucleus
IMD	intermediodorsal thalamic nucleus
ic	internal capsule
IF	interfascicular nucleus
IP	interpeduncular nucleus
LA	lateroanterior hypothalamic nucleus
LC	locus coeruleus
LD	laterodorsal thalamic nucleus
LDT	laterodorsal tegmental nucleus
Lh	lateral habenula
LH	lateral hypothalamic area
lfp	longitudinal fasciculus of the pons
ll	lateral lemniscus
lo	lateral olfactory tract
LOT	nucleus of the lateral olfactory tract
LP	lateral posterior thalamic nucleus
LPB	lateral parabrachial nucleus
LPO	lateral preoptic area
LSO	lateral superior olive
LV	lateral ventricle
m5	motor root of the trigeminal nerve
mcp	middle cerebellar peduncle
MD	mediodorsal thalamic nucleus
MDl	mediodorsal thalamic nucleus, lateral part
MDm	mediodorsal thalamic nucleus, medial part
ME	median eminence
Me	medial amygdaloid nucleus
Med	medial amygdaloid nucleus, anterodorsal part
Mev	medial amygdaloid nucleus, anteroventral part
MG	medial geniculate nucleus
Mh	medial habenula
ml	medial lemniscus
mlf	medial longitudinal fasciculus
MM	medial mammillary nucleus, medial part
MnR	median raphe nucleus
Mo5	motor trigeminal nucleus
mp	mammillary peduncle
MPA	medial preoptic area
MPB	medial parabrachial nucleus
mPFC	medial prefrontal cortex
MPO	medial preoptic nucleus
MS/VDB	medial septum/vertical limb of the diagonal band of Broca
MSO	medial superior olive
mt	mammillothalamic tract
MT	medial terminal nucleus of the accessory olfactory tract
MTu	medial tuberal nucleus
OVL	organum vasculosum of the lamina terminalis
ot	optic tract
ox	optic chiasm
PAG	periaqueductal gray
Pap	paraventricular hypothalamic nucleus, parvicellular part
PBG	parabigeminal nucleus
PC	paracentral thalamic nucleus
pc	posterior commissure
PeF	perifornical nucleus
PI	posterior group of intralaminar thalamic nuclei
Pir	piriform cortex
PF	parafascicular thalamic nucleus
PH	posterior hypothalamic area
PMD	premammillary nucleus, dorsal part
PMV	premammillary nucleus, ventral part
Pn	pontine nuclei
Po	posterior thalamic nuclear group
PPT	pedunculopontine tegmental nucleus
Pr5	principle sensory trigeminal nucleus
PT	paratenial thalamic nucleus
PVH	paraventricular hypothalamic nucleus, magnocellular part
py	pyramidal tract
R	red nucleus
Re	reuniens thalamic nucleus
Rh	rhomboid thalamic nucleus
RPa	raphe pallidus nucleus
RPO	rostral periolivary nucleus
Rt	reticular thalamic nucleus
RtTg	reticulotegmental nucleus of the pons
S1	primary somatosensory cortex
SCO	subcommissural organ
SCh	suprachiasmatic nucleus
sc	superior cerebellar peduncle
SFi	septofimbrial nucleus
SFO	subfornical organ
SI	substantia innominata
sm	stria medularis
SNc	substantia nigra, compact part
SNr	substantia nigra, reticular part
SO	supraoptic nucleus
st	stria terminalis
STh	subthalamic nucleus
Sub	submedius thalamic nucleus
SubI	subincertal nucleus
SuG	superficial gray of the superior colliculus
TM	tuberomammillary nucleus
TS	triangular septal nucleus
Tu	olfactory tubercle
Tz	nucleus of the trapezoid body
VA	ventral anterior thalamic nucleus
VB	ventrobasal thalamic nuclei
VE	ventral endopiriform nucleus
Vglut	vesicular glutamate transporter
VL	ventrolateral thalamic nucleus
VLG	ventral lateral geniculate nucleus
VM	ventromedial thalamic nucleus
VMH	ventromedial hypothalamic nucleus
VP	ventral pallidum
VPM	ventral posteromedial thalamic nucleus
VPL	ventral posterolateral thalamic nucleus
VPpc	ventral posterior thalamic nucleus, parvicellular part
VTA	ventral tegmental area
VTg	ventral tegmental nucleus
Xi	xiphoid thalamic nucleus
ZI	zona incerta

2002; Schafer et al., 2002; Fremeau et al., 2002; Harkany et al., 2004; Herzog et al., 2004; Somogyi et al., 2004).

Subcortical regions known to project to the neocortex contain Vglut2 neurons. However, the contribution of Vglut2-containing neurons to corticopetal projection has not been described. Therefore, the purpose of this study was to determine the distribution of neocortically projecting Vglut2 neurons. We chose to investigate the Vglut2 cells projecting to two functionally distinct cortical areas, the medial prefrontal and primary somatosensory cortices (mPFC and S1, respectively). In situ hybridization techniques were used to reveal the location of Vglut2 cell bodies following retrograde tracer injections of Fluoro-Gold into the mPFC and S1. In order to estimate the Vglut2 contribution to these cortical areas from the extrathalamic pool of Vglut2, we first describe the distribution of Vglut2 cells in extrathalamic subcortical areas in some detail. A preliminary material of this study was published in abstract form (Hur et al., 2002).

MATERIALS AND METHODS

Eight male Sprague-Dawley rats (270–300 g; Zivic Miller Laboratories, Portersville, PA) were housed individually and maintained on a 12-hour light/dark cycle with water and food as desired. Six rats were used for combined retrograde tracer and in situ hybridization and two rats were processed for in situ hybridization only. All experiments were performed in accordance with the National Institutes of Health *Guidelines for the Care and Use of Animals in Research* and approved by the Rutgers University Institutional Review Board.

Injections of retrograde marker Fluoro-Gold (FG)

To identify cortically projecting neurons, the retrograde tracer FG (4%, Fluorochrome, Englewood, CO) was injected into either the mPFC or S1. First, rats were deeply anesthetized with a mixture of ketamine (80 mg/kg) and xylazine (15 mg/kg) administered intraperitoneally. Rats were then placed into a stereotaxic frame with bregma and lambda leveled. All wound margins and points of contact between the animal and the stereotaxic apparatus were infiltrated with lidocaine solution (2%) and xylocaine ointment (5%), respectively. Using aseptic techniques, the scalp and overlying fascia were retracted from the skull and small burr holes were drilled over mPFC or S1. FG was pressure injected (0.3 μL) into the medial prefrontal cortex (AP +3.7, ML +0.4, DV –3.0; AP +3.2, ML +0.5, DV –3.0; AP +2.7, ML +, DV –) or primary somatosensory cortex (AP 1.6, ML +4.6, DV –2.8; AP +1.0, ML +3.8, DV –1.7; AP +0.3, ML +3.2, DV –1.4) of the right hemisphere. Following surgery, the scalp was closed and betadine was administered. Rats with cortical injections of FG were allowed to survive 7–10 days.

All rats were given a lethal dose of urethane (2.8 g/kg, i.p.) and perfused transcardially with 100 ml of phosphate-buffered saline (PBS, pH 7.4) followed by 400 mL of 4% paraformaldehyde (Electron Microscopy Sciences, Fort Washington, PA) in 0.1 M sodium phosphate buffer, pH 7.4 The brains were removed and stored in fixative at 4°C overnight. Coronal sections (30 μm) were cut with a vibrating microtome and collected in six series into sterile PBS.

Preparation of digoxigenin-labeled RNA riboprobe for detection of Vglut2 mRNA

The antisense riboprobe for rat Vglut2 was transcribed from a 1,119 bp DNA template (Stornetta et al., 2002) inserted into the TOPO cloning site of pCRII-TOPO (Invitrogen, Carlsbad, CA) in an in vitro polymerization reaction using SP6 RNA polymerase (Promega, Madison, WI) and digoxigenin-11-UTP (Roche Molecular Biochemicals, Indianapolis, IN). The efficiency of digoxigenin-11-UTP incorporation was estimated by direct immunological detection on dot blots using a sheep polyclonal anti-digoxigenin antibody (Roche Molecular Biochemicals).

Histochemistry

All histochemical procedures were performed using free-floating sections rinsed in sterile PBS (pH 7.4) and transferred into prehybridization solution at room temperature for 30 minutes, then at 37°C for 1 hour. The prehybridization mixture consisted of 0.6 M NaCl, 0.1 M Tris-Cl, pH 7.5, 0.01 M ethylenediamine tetraacetic acid (EDTA), 0.05% $NaPP_i$, 0.5 mg/ml yeast total RNA, 0.05 mg/ml yeast tRNA, 1× Denhardt's bovine serum albumin, 50% formamide, 15% dextran sulfate, 0.05 M poly-A, 10 μM of the four deoxynucleoside triphosphates, 0.5 mg/ml herring sperm DNA, and 10 mM dithiothreitol. The riboprobes were added directly to the prehybridization solution containing the sections at a concentration of 50–100 pg/μl. Some sections were incubated with sense Vglut2 riboprobe at a matched concentration as a control. Sections were incubated with riboprobe at 55–60°C for 16-20 hours, followed by rinses through decreasing concentrations of salt solutions (lowest salt concentration at 55°C for 1 hour) and treatment with RNAse A (20 μg/ml, Sigma, St. Louis, MO). Sections were incubated in 10% normal horse serum with 0.1% Triton X-100 for 30 minutes, then transferred to a sheep anti-digoxigenin antibody conjugated to alkaline phosphatase (1:1,000; Roche Molecular Biochemicals) in 10% normal horse serum and 0.1% Triton X-100 overnight at 4°C. The alkaline phosphatase was reacted with nitroblue tetrazolium and 5-bromo-4-chloro-3-indolyl-phosphate,4-toluidine salt. Absence of labeling in the striatum and reticular thalamic nuclei was observed under a dissecting microscope as the colorization reaction proceeded. The reaction was quenched with three 10-minute rinses in 0.1 M Tris / 1 mM EDTA, pH 8.5. The appropriate reaction time was defined by the appearance of signal in the absence of or with minimal striatal neuron labeling. The maximal tolerated background was a thin perinuclear rim of reaction product that was easily distinguishable from the denser and homogeneous filling (but sparing the nucleus) of neuronal cell bodies considered to be positively labeled.

Because the in situ hybridization protocol may attenuate FG fluorescence, FG was detected immunohistochemically using a rabbit polyclonal antibody (Chemicon, Temecula, CA; 1:5,000; overnight at 4°C), followed by antirabbit IgG conjugated to indocarbocyanine (Cy3; 1:200; 1 hour; Jackson ImmunoResearch Laboratories, West Grove, PA). After rinsing in TBS, the sections were mounted in rostrocaudal order onto slides and dried. The coverslips were affixed with Vectashield (Vector, Burlingame, CA) and the edges sealed with nail polish. No label was observed in the absence of the primary antibody.

TABLE 1. Mapped Vglut2 Neurons in Forebrain Structures from 3 Brains

Structure[1]	Vglut2 cells mapped	Volume mapped, 10^7 μm^3	Vglut2 cells/ 10^7 μm^3	Vglut2 cells/section ± SEM[2]
MS/VDB (6)	742	9.543	78	123.4 ± 30.3[a,b,c]
HDB (9)	768	5.188	148	85.3 ± 6.0[d,e,f]
VP (9)	365	12.445	29	40.6 ± 11.9[g,h,i]
SI (15)	1,354	14.430	94	90.3 ± 21.1[j,k,l]
GP (15)	138	26.780	5	9.2 ± 3.2
ic (20)	694	51.976	13	34.7 ± 9.6
BSt (9)	471	10.859	43	52.3 ± 26.6
MPO (8)	1,003	4.236	237	125.4 ± 29.6
LA (4)	414	0.919	450	103.5 ± 28.8
ADP (3)	173	0.752	230	57.7 ± 20.2
AHA (7)	954	3.205	298	136.3 ± 48.2
LPO (6)	617	5.103	121	102.8 ± 30.5
LH (17)	4,659	21.144	12,122	274.1 ± 31.1[a,d,g,j]
PVH (8)	1,168	2.105	555	146.0 ± 27.7
VMH (8)	5,353	4.415	1,212	669.1 ± 70.4[b,e,h,i]
DMH (4)	1,133	2.060	550	283.3 ± 74.5
PH (6)	3,042	4.309	706	507.0 ± 113.6[c,f,i,l]
LOT (6)	2,478	2.817	850	413.00 ± 54.3
Me (10)	3,818	5.436	702	381.80 ± 65.4
Ce (6)	13	3.991	3	2.2 ± 1.1
BL (6)	11	40.134	3	1.8 ± 1.1
La (6)	0	2.110	0	0 ± 0
ACo (9)	1,236	2.788	443	137.2 ± 32.7
BM (8)	2,106	2.708	778	263.25 ± 76.9

[1]Number of mapped sections for each brain structure is indicated in parentheses.
[2]Same superscript letters denote significant differences between corresponding structures.

Data analysis

Three brains for each injection location (mPFC or S1) were mapped. The outlines and major landmarks of the sections of interest were drawn with a 5× lens under darkfield illumination using a motor-driven microscope stage controlled by the Neurolucida software package (MicroBrightField, Williston, VT). The location of labeled cell bodies was mapped using a 20× objective under fluorescence or brightfield illumination as required. Major forebrain areas/nuclei were delineated using standard cytoarchitectonic criteria (Paxinos and Watson, 1998). Darkfield illumination was used to facilitate the delineation of fiber bundles. Ventral thalamic nuclei delineation was according to Faull and Carman (1978). Cell groups within the "a and b" components of the medial forebrain bundle were termed the horizontal limb of the diagonal band (HDB) according to Zaborszky et al. (1986) rather than subdelineating the region medially as HDB and laterally as the magnocellular preoptic nucleus (Paxinos and Watson, 1998). Single retrograde and double-labeled neurons within defined brain regions were counted and Vglut2 cells were mapped in all forebrain areas except the thalamus. By focusing on the top and bottom of the mounted sections and recording the Z-axis coordinates provided by Neurolucida, we measured the thickness of the mapped sections (ranging from 6.9–16.1 μm). The surface area of delineated brain regions was measured using NeuroExplorer (MicroBrightField). The number of Vglut2 cells per mapped volume (Vglut2 cell density) was expressed in 10^7 μm^3. The mean and standard error of the mean of Vglut2 cells/section were calculated. The mapped volume was obtained by multiplying the measured section thickness with the mapped surface area (Table 1).

To extrapolate the total number of double-labeled cells in individual brain structures, we used the original cut section thickness (30 μm), average surface area of a given brain structure per section, the anteroposterior distance of the structure using a rat brain atlas (Paxinos and Watson, 1998), and the average number of Vglut2 and double-labeled cells per section according to the following equations (Table 2).

TABLE 2. Estimates of Cells Vglut2 and Vglut/FG Following mPFC Injection in Selected Brain Structures Corrected for the Living State[1]

Structure	Total volume, μm^3	Vglut2 cells	Double-labeled cells
MS/VDB	1,169,220,912	4,234	48
HDB	1,232,158,497	3,533	30
SI	1,270,982,614	3,233	33
VP	1,560,698,042	1,404	30
VMH	537,718,480	22,603	113
LH	2,802,183,000	24,522	222
PH	662,195,760	13,040	104

[1]Calculated using 30 μm section thickness, average mapped section surface area, and anterior–posterior distance from the atlas (Paxinos and Watson, 1998; See Materials and Methods for details).

$$V = \Sigma F/N \times h \quad (1)$$

The volume of a given brain structure (V) was calculated from the total mapped surface area of a given structure (ΣF) divided by the number of sections (N) multiplied by anterior-posterior distance (h) of the structure in the Paxinos-Watson atlas (1998).

$$N_T = V/[(\Sigma F/N) \times 30] \quad (2)$$

The theoretical number of sections (N_T) in a given volume was calculated according to Eq. [2] using 30-μm section thickness.

$$Q_T = N_T \times (Q^-/N) \quad (3)$$

The number of Vglut2 cells (Q_T) in Table 2 was calculated according to Eq. [3], where Q^- is the total number of mapped cells.

The number of double-labeled, single retrograde, and single-labeled Vglut2 neurons is reported for each extrathalamic mapped brain region (Tables 3, 4). A more detailed dataset of forebrain and brainstem areas for Case 35 (prefrontal cortex injection) and the thalamus of Case 01 (primary somatosensory cortex injection) are provided in Tables 5 and 6. Student's *t*-test was used to compare cell counts between prefrontal and somatosensory cortically injected rats. Kruskal-Wallis test was used to compare populations with large variances. The 95% confidence intervals were determined for seven structures labeled with superscripts in Table 1.

Digital image processing

Neurolucida files were exported to Adobe Illustrator (v. 8.0; Adobe Systems, Mountain View, CA). Photo images were obtained with an Axiocam digital camera (Zeiss Axioskop; resolution 3900 × 3090 pixels) and the resulting TIFF files were imported into Adobe PhotoShop. Output levels were adjusted to include information-containing pixels. Color balance and contrast were adjusted to reflect true color as much as possible.

RESULTS

Distribution of Vglut2 cells in forebrain areas

Figures 1 and 2 and 6C are low-magnification digital photomontages of rostrocaudal coronal sections processed

TABLE 3. Retrograde Cell Counts from Rats Receiving Prefrontal Cortex Injection[1]

Structure	Case 02 7.20 × 10^4 μm^3		Case 35 13.22 × 10^6 μm^3		Case 37 9.28 × 10^6 μm^3		Total[2] double	Total[2] single	Total retrograde[2]	% Double-labeled cells[3]
	Double	Single	Double	Single	Double	Single				
Basal forebrain	9	281	24	286	2	94	35	661	696	0.43
Hypothalamus	178	462	117	43	16	33	311	538	849	3.81
Claustrum	46	212	169	398	124	120	339	730	1,069	4.15
Amygdala	32	2,124	4	384	5	495	41	3,003	3,044	0.50
Pir. cortex	1	5,189	8	996	4	193	13	6,378	6,391	0.16
Thalamus	4,726	11	1,526	16	1,117	4	7,369	31	7,400	90.22
Brainstem	—	—	37	285	23	80	60	365	425	0.73
Total	4,992	8,279	1,885	2,408	1,291	1,019	8,168	11,706	19,904	100.00

[1]Injection volumes are indicated below each case number.
[2]Sum of cells in a given structure from all three cases.
[3]Percentage of double-labeled cells in a structure from the total number of double-labeled cells from all structures.

TABLE 4. Retrograde Cell Counts from Rats Receiving Somatosensory Injection[1]

Structure	Case 01 15.01 × 10^6 μm^3		Case 34 12.13 × 10^6 μm^3		Case 68 14.24 × 10^6 μm^3		Total[2] double	Total[2] single	Total[2] retrograde	% Double-labeled cells[3]
	Double	Single	Double	Single	Double	Single				
Basal forebrain	4	217	20	126	3	213	27	556	583	0.39
Hypothalamus	14	45	5	10	2	30	21	85	106	0.30
Claustrum	123	124	1	3	79	219	203	346	549	2.92
Amygdala	0	226	0	79	8	4,347	8	4,652	4,660	0.11
Pir. cortex	0	176	0	60	0	60	0	296	296	0.00
Thalamus	2,780	8	715	5	3,202	0	6,697	13	6,710	96.18
Brainstem	—	—	7	73	—	—	7	73	80	0.10
Total	2,921	796	748	356	3,294	4,869	6,963	6,021	12,984	100.00

[1]Injection volumes are indicated below each case number. 2
[a]Sum of cells in a given structure from all three cases.
[3]Percentage of double-labeled cells in a structure from the total number of double-labeled cells from all structures.

for Vglut2 mRNA to show the distribution of Vglut2 cells in the forebrain. Additionally, Figures 4–7 display the distribution of Vglut2 cells in extrathalamic forebrain areas and corticopetal Vglut2 projection neurons to the mPFC.

Septum and diagonal band nuclei. In general, the density of Vglut2 cells in the medial septum/vertical limb of the diagonal band of Broca complex (MS/VDB) is sparse, except in its most rostral area at about 1.0 mm anterior to bregma (Figs. 1A, 4A; Table 1). Ventrally, where the diagonal band approaches the brain surface, a few labeled cells are observed (Figs. 1B, 4B). On the other hand, at about 0.2 mm anterior to bregma, labeled cells tend to be located lateral to the MS/VDB (Fig. 1B), corresponding to an area termed the paralambdoid septal nucleus (Paxinos and Watson, 1998). These neurons appear to continue into the septofimbrial nucleus (Fig. 1C, 4C) that is heavily populated by Vglut2 cells. Scattered Vglut2 cells are observed also in other parts of the septum, including its dorsal and lateral parts. A moderate number of Vglut2 cells is diffusely distributed in the horizontal limb of the diagonal band of Broca (HDB) in its entire rostrocaudal extent (Figs. 1B, 2C, 4C, 5D; Table 1).

Pallidal structures and the internal capsule. Vglut2 cells are scarcely distributed in the ventral pallidum. A peculiar group of large multipolar cells accumulate in the dorsal-medial part of the ventral pallidum at about 0.2 mm anterior to bregma, apparently in continuity with the Vglut2 cells in the intermediate septal group rostrally (Fig. 1B, asterisk) and caudally, just behind the crossing of the anterior commissure, in the caudomedial part of the ventral pallidum (Figs. 1C, 4C). A few heavily labeled cells are located in the ventral part of the globus pallidus (Fig. 1D, asterisk); this group may be in continuity with the heavily labeled Vglut2 cell cluster in the ventral pallidum. Scattered small-to-medium-sized labeled cells are also in the ventral and caudal parts of the globus pallidus (Fig. 5A,B). There are only few labeled cells in the rostral part of the internal capsule (Figs. 1D, 2A,B, 5A–D). However, a large number of Vglut2 cells infiltrates the internal capsule beginning at about 2 mm caudal to bregma, corresponding to the entopeduncular nucleus (Figs. 2C, 5C,D).

Substantia innominata and bed nucleus of the stria terminalis. Vglut2 cells in the substantia innominata appear rather inconspicuously rostrally between the lateral part of the VDB/HDB and the medial part of the ventral pallidum (Fig. 4B,C). More caudally, where the substantia innominata increases in size, labeled cells in this structure continue to be inserted between the globus pallidus dorsally and the HDB ventrally (Figs. 1D, 4D, 5A). More caudal areas of the substantia innominata display loosely arranged cells just underneath the internal capsule and globus pallidus (Figs. 2B,C, 5B). Further caudally, a narrow band of Vglut2 cells is located ventral to the internal capsule, extending toward the globus pallidus that represents the caudal portion of the substantia innominata (Figs. 2C, 5C). The Vglut2 cell density and estimated cell numbers in the substantia innominata are similar to those of the MS/VDB (Tables 1, 2). At the level of the crossing of the anterior commissure, Vglut2 labeled cells appear in the anterior medial subdivision of the bed nucleus of the stria terminalis, while the lateral part is devoid of Vglut2 cells (Fig. 1C). More caudally, there is a conspicuous group of heavily labeled cells in an intermediate position (Fig. 1D). At the same level, there is also a

TABLE 5. Double-Labeled Cells Following FG Injection to Prefrontal Cortex Case 35

	DL cells	Single FG	Single Vglut2
Basal forebrain			
MS/VDB	5	52	375
VP	4	81	189
BSt	1	5	354
SI	7	70	228
Septofimbrial nucleus	1	0	69
HDB	4	27	321
ic	2	16	122
GP	0	35	78
Total	24	286	1,736
Amygdala			
ACo	2	1	411
Me	0	1	607
BM	2	80	223
Ce	0	1	11
BL	0	272	11
La	0	29	0
Total	4	384	1,263
Hypothalamus			
MPO	5	1	1070
ADP	0	0	64
AH	2	0	462
SCN	0	0	0
SON	0	0	101
Arc	0	0	146
VMH	12	3	1,175
DMH	3	3	359
PMV	2	1	360
PeF + fornix	13	22	128
LH	32	1	1,839
LPO	3	5	230
Tuber cinereum	14	7	144
PH	23	0	467
MTu	3	0	158
MM	0	0	356
SuM	0	0	218
ML	0	0	266
TM	5	0	73
Total	117	43	7,616
Piriform			
DEndopiriform	5	319	48
VEndopiriform	0	4	102
Piriform cortex	3	673	283
Total	8	996	433
Subthalamic Area			
ZI	3	0	21
STh	0	0	256
Total	3	0	277
Claustrum	169	398	437

Thalamus	DL Cells	Single FG
PC, CM, CL	196	1
Re	176	0
Rh	34	0
PF	0	0
F. retroflexus	4	0
PT	130	4
PVA	115	0
PVP	29	1
IMD	74	0
MD	335	7
AD	4	0
AV	6	0
AM	151	0
IAM	103	1
VA	21	0
VL	2	0
VM	127	1
LD	1	0
LP	1	0
RI	0	0
sc	1	0
Rt	0	1
Sub	14	0
VPL	0	0
VPM	1	0
VLG	0	0
Gustatory	1	0
Total	1,526	16
Brainstem		
PAG	1	15
ml	0	5
mkf	1	1

TABLE 5. Continued

	DL Cells	Single FG
Brainstem		
CLi	4	3
MT	0	4
sc	0	1
VTA	8	14
MnR	0	17
SNr	0	2
DR	0	23
LDT	1	14
PB	0	2
DT	0	1
PnR	0	1
LC	0	25
Other	22	157
Total	37	285

TABLE 6. Double-Labeled Cells in the Thalamus Following FG Injection to the Somatosensory cortex (Case 01)

Thalamus	DL Cells	Single FG
PC, CM, CL	97	0
Re	6	1
Rh	46	2
PF	3	0
PT	0	0
PVA	0	0
PVP	0	0
IMD	8	0
MD	23	0
AD	93	0
AV	475	0
AM	7	0
IAM	0	0
VA	29	0
VL	328	0
VM	36	4
LD	169	0
LP	45	0
Po	411	0
Rt	2	0
Sub	0	0
VPL	720	0
VPM	279	0
DLG	3	1
Total	2,780	8

thin sheet of cells in its medialmost border, towards the fornix (Figs. 1D, 4D). Scattered labeled cells are located in the most caudal part of this nucleus, around the fornix (Figs. 2A,B, 5A).

Medial preoptic / medial hypothalamic areas. In agreement with Ziegler et al. (2002) and Lin et al. (2003), many Vglut2 cells are seen in the preoptic region, including the median, periventricular, anterodorsal, and medial preoptic nuclei (Figs. 1C,D, 4C,D). Within the anterior hypothalamic area the lateroanterior nucleus is densely populated by Vglut2 cells, while the rest of this region, especially in its medial part, contains only a few scattered labeled cells (Figs. 2A, 5A). The suprachiasmatic nucleus is free of labeled cells (Fig. 2A). The Vglut2 cell density of the magnocellular and parvicellular subdivisions of the paraventricular hypothalamic nucleus is moderately high (Table 1) but the majority of these cells are only weakly stained (Fig. 2A,B). The ventromedial hypothalamic nucleus along its rostrocaudal extent massively expressed Vglut2 mRNA (Figs. 2C,D, 5C,D), and it has the highest Vglut2 cell density among the investigated areas (Table 1). The central (so-called "compact") compartment of the dorsomedial hypothalamic nucleus shows stronger Vglut2 staining than its dorsal and ventral compartments (Figs. 2D, 5D). The arcuate nucleus only contains a few Vglut2 cells, mostly in its lateral part (Figs. 2C,D, 5D). The pos-

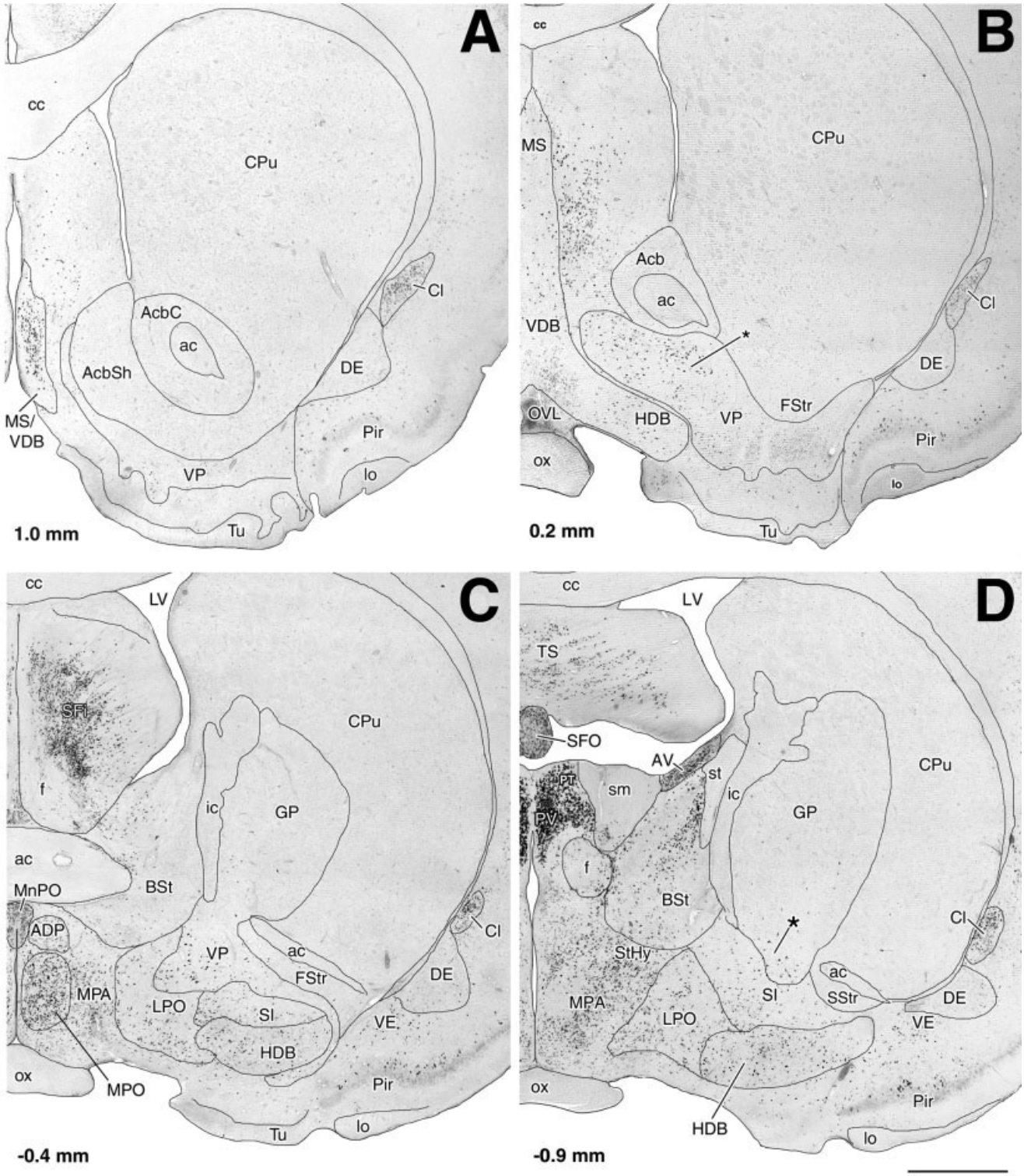

Fig. 1. Digital photomontages of forebrain areas containing cells expressing Vglut2. Neurons expressing Vglut2 are located in the MS/VDB and the claustrum (Cl), piriform cortex (Pir), and ventral endopiriform nucleus (VE). In contrast, the striatum (CPu) and dorsal endopiriform nucleus (DE) contain very few Vglut2 neurons. **A:** The core (AcbC) and shell (AcbSh) of the nucleus accumbens are relatively free of Vglut2-expressing cells. **B:** Vglut2 cells are observed lateral to the medial septum (MS). Note the abundance of darkly stained Vglut2 cells in the dorsal ventral pallidum (VP, asterisk). **C:** Vglut2 expression occurs in the septofimbrial nucleus (SFi), preoptic nuclei (ADP, MPA, MPO, LPO), substantia innominata (SI), and horizontal limb of the diagonal band of Broca (HDB). **D:** The paraventricular (PV), paratenial (PT), and anteroventral (AV) thalamic nuclei contain densely stained neurons. Note the small population of darkly stained Vglut2 cells in the ventral portion of the globus pallidus (GP, asterisk). Bregma levels are indicated for each panel. Scale bar = 1 mm.

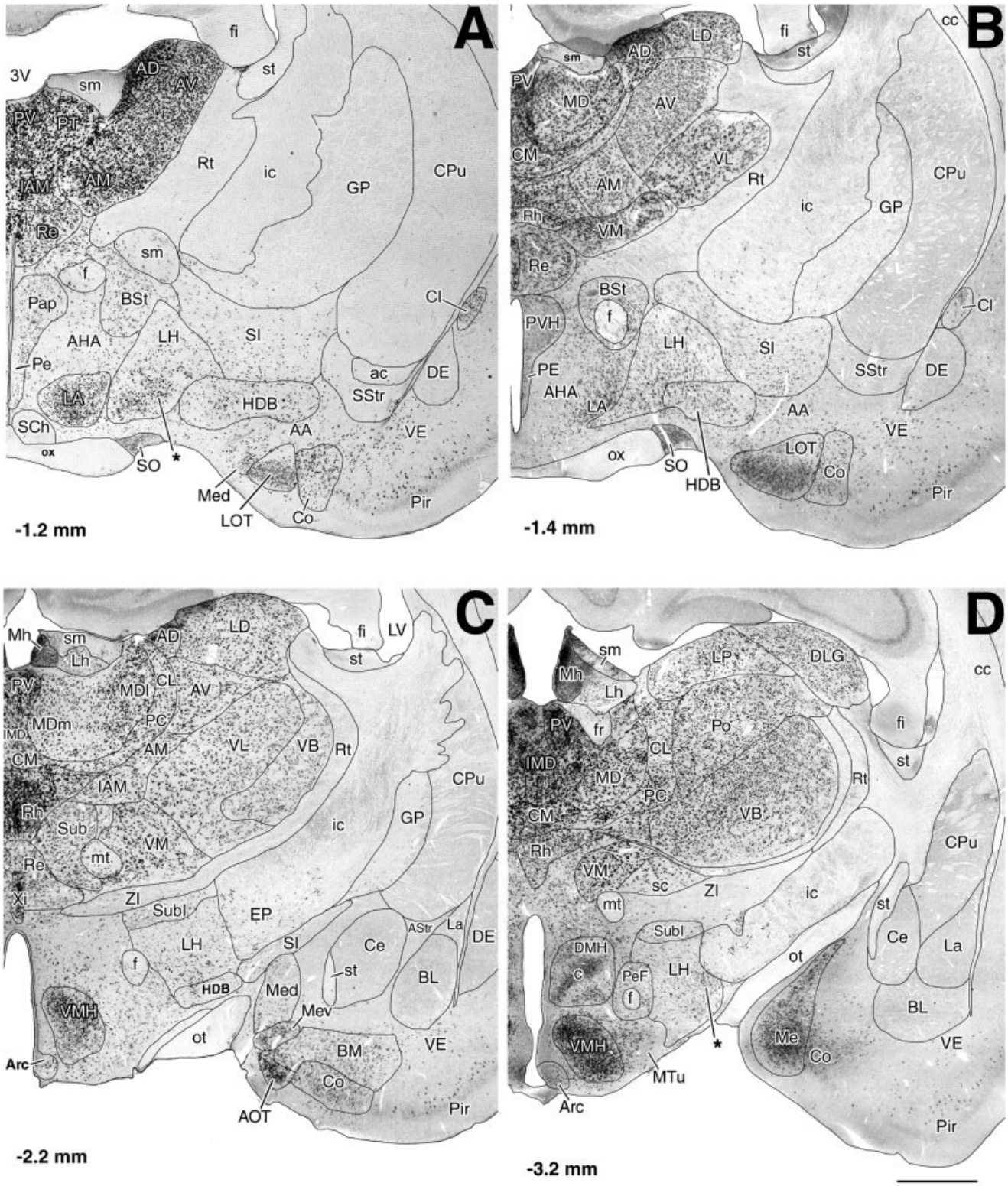

Fig. 2. Digital photomontages of caudal forebrain areas containing cells expressing Vglut2. With the exception of the reticular thalamic nucleus (Rt), thalamic nuclei are rich in Vglut2 cells. Vglut2 expression is also seen in several hypothalamic and basal forebrain areas, the claustrum (Cl), and ventral endopiriform nucleus (VE). **A,B:** The lateroanterior hypothalamic nucleus (LA) and lateral hypothalamic area (LH) are rich in Vglut2 cells. Vglut2-expressing cells are scattered in the substantia innominata (SI), the ventral part of the internal capsule (ic), and HDB. In the amygdala, Layer II of the nucleus of the lateral olfactory tract (LOT), the anterior amygdaloid area (AA), and the anterior cortical nucleus (Co) contain Vglut2. The supraoptic nucleus (SO) and paraventricular hypothalamic nucleus (PVH) are positive for Vglut2, but the suprachiasmatic (SCh) nucleus is devoid of Vglut2 expression. **C,D:** The midline thalamic nuclei are strongly stained for Vglut2, particularly the paraventricular (PV), central medial (CM), and rhomboid (Rh) thalamic nuclei. The ventromedial hypothalamic nucleus (VMH) has the highest Vglut2 cell density in the forebrain (see text and Table 1). Vglut2 expression is moderate in the LH, HDB, entopeduncular nucleus (EP), and SI. The globus pallidus (GP) contains very little Vglut2 mRNA. The basomedial (BM), bed nucleus of the accessory olfactory tract (AOT), anterior cortical (Co), and the ventral part of the medial amygdaloid nucleus (Mev) are strongly labeled. D: The lateral hypothalamus (LH) has clusters of Vglut2 cells in its lateral part (asterisk). Note that the central (compact) part of the dorsomedial hypothalamic nucleus (DMH, c) is rich in Vglut2 expression as well. Scale bar = 1 mm.

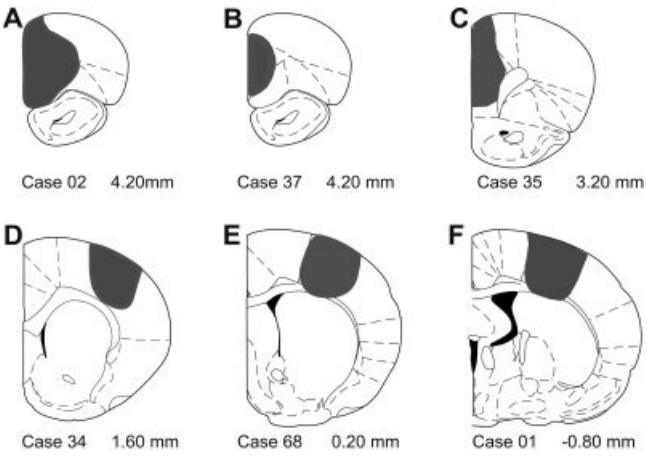

Fig. 3. Retrograde tracer injection sites in the medial prefrontal (**A–C**) and primary somatosensory (**D–F**) cortices are shown at the level of their largest extent. Case numbers and corresponding bregma levels are indicated below each brain.

terior hypothalamic area contains strong Vglut2 staining (Fig. 6A–C). The dorsal and ventral premammillary nuclei have moderately high Vglut2 cell density and staining (Fig. 6A,B). The rostral part of the medial mammillary nucleus is especially rich in Vglut2 cells (Fig. 6B). There are a few lightly labeled cells in the lateral mammillary nucleus (not shown).

Lateral preoptic / lateral hypothalamic areas. Loosely arranged cells in the entire rostrocaudal extent of the lateral preoptic/hypothalamic areas show moderate Vglut2 staining. At the level of the suprachiasmatic nucleus, dorsal to the supraoptic nucleus, a heavily stained group of multipolar cells appears prominently in the ventromedial part of the lateral hypothalamic area (Fig. 2A). More caudally, these cells blend into the caudal aspect of the HDB (Fig. 2B,C). Occasionally, labeled cells form clusters (Fig. 2A, asterisk). Such clusters are also observed laterally, near the internal capsule in a region called the magnocellular nucleus of the lateral hypothalamus in the Paxinos-Watson atlas (Fig. 2D, asterisk). Loosely arranged labeled cells surround the fornix at midcaudal hypothalamic levels corresponding to the perifornical nucleus (Figs. 5D, 6A). Caudally, numerous labeled cells are visible underneath the fornix between the ventromedial hypothalamic nucleus and lateral hypothalamic area and may correspond to the medial tuber nucleus (Figs. 5D, 6A) of Paxinos and Watson (1998). A few cells in the tuberomammillary nucleus exhibit weak Vglut2 staining (Fig. 6B).

Subthalamic regions. The zona incerta is mostly free of Vglut2 cells. However, a few labeled cells are encountered in its medial part, around the mammillothalamic tract at ~3.5 mm caudal to bregma (Figs. 2D, 6A–C). There are few Vglut2 neurons diffusely positioned throughout the fields of Forel (F in Figs. 6B, 6C). There are numerous Vglut2 cells ventral to the zona incerta, in the subincertal nucleus, dorsal to the lateral hypothalamic area (Figs. 2C,D, 5D). The subthalamic nucleus is strongly stained with Vglut2 and is clearly visible on the dorsomedial aspect of the internal capsule (Fig. 6A,C).

Amygdala. The anterior amygdaloid area has few scattered Vglut2 cells (Figs. 2B, 4D, 5A). In contrast, the nucleus of the lateral olfactory tract contains a dense group of strongly labeled Vglut2 cells primarily in its Layer 2 (Figs. 2A,B, 5A,B). The bed nucleus of the accessory olfactory tract also exhibits dense staining (AOT in Figs. 2C, 5C). The basomedial nucleus expresses a medium-to-high amount of Vglut2 mRNA (Fig. 2C). The dorsal part of the medial amygdaloid nucleus has light to moderate Vglut2 staining, whereas the ventral part was denser and had darker staining in its rostral division (Fig. 2C). More caudally, Vglut2 is darker and abundant both dorsally and ventrally in the medial amygdaloid nucleus (Figs. 2D, 5D). Interestingly, we did not detect Vglut2 cells in the lateral, basolateral, and central amygdaloid nuclei (Figs. 2C,D, 5B–D). The periamygdaloid cortical areas contains a moderate amount of Vglut2 cells (Co in Figs. 2B–D, 5A–C, Table 1).

Claustrum, piriform cortex, and endopiriform nuclei. The claustrum, visible between +1.20 to –1.85 from bregma, is filled by a large number of moderately intense Vglut2 cells (Figs. 1, 2A,B, 4, 5A–C). Few strongly labeled Vglut2 positive cells can be seen throughout its entire rostrocaudal extent, both in Layers IIb and III of the piriform cortex (Figs. 1, 2, 4, 5). The dorsal endopiriform nucleus contains few lightly labeled Vglut2 cells (Figs. 1D, 4C). The ventral endopiriform nucleus contains a small proportion of strongly labeled Vglut2 cells throughout its rostrocaudal extent (Figs. 1, 2, 4, 5).

Vglut2 cell density and estimated cell numbers

According to our estimations, the ventromedial hypothalamic nucleus has the highest Vglut2 cell density among extrathalamic areas (~670 cells/section). High-density distribution of Vglut2 cells was found in several amygdaloid (e.g., nucleus of the lateral olfactory tract, 413 cells/section) and hypothalamic nuclei (e.g., posterior hypothalamic area, 507 cells/section). Medium-density areas include the medial preoptic nucleus (125 cells/section). Basal forebrain areas, including MS/VDB, HDB, and substantia innominata have a low-to-medium density of Vglut2 cells (40–123 cells/section). For comparison, the estimated total number of Vglut2 cells adjusted to the living state is listed for selected areas of the basal forebrain and hypothalamus in Table 2. The density of Vglut2 cells is significantly higher in individual hypothalamic structures than in the investigated basal forebrain areas (superscripts in Table 1).

Distribution of retrograde and double-labeled cells following prefrontal cortex injections

Retrograde tracer injection sites (Fig. 3) and cell counts (Table 3). Retrograde tracer injections into the medial prefrontal cortex were analyzed from Cases 02, 35, and 37 (Fig. 3). The detailed maps in Figures 4 and 5 are from the representative Case 35. All prefrontal injections included the prelimbic, infralimbic, and the dorsal cingulate area (Cg1; Paxinos and Watson, 1998). In addition, in Case 02 the medial, ventral and the rostrolateral orbital areas, the dorsal tenia tecta, and the medial part of the secondary motor cortex were labeled. About 35% of all (n = 23,081) cells projecting to the mPFC also expressed Vglut2 (Table 3). Of all double-labeled cells, the thalamus provided 90%. The rest comes from the claustrum (4.2%),

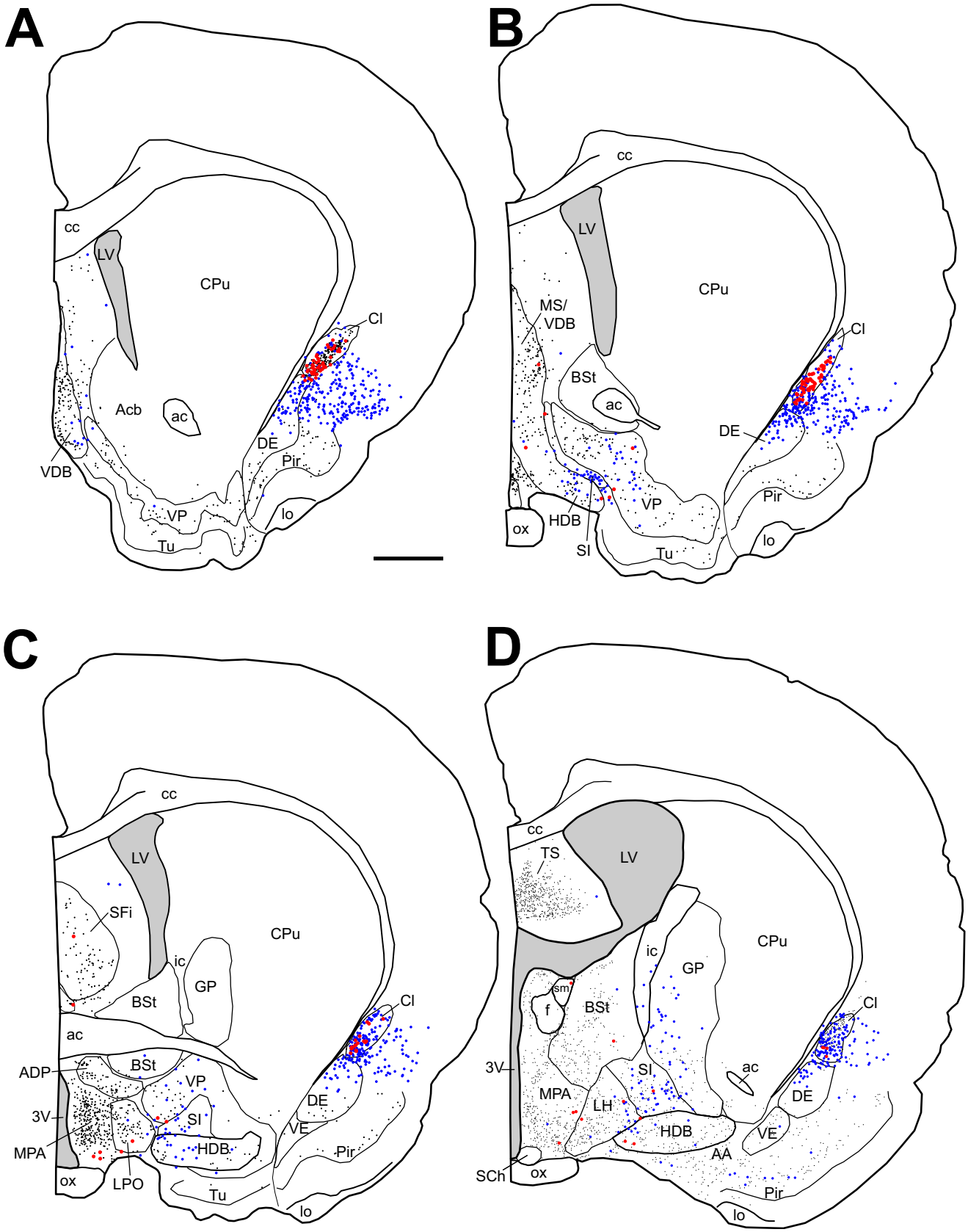

Fig. 4. Distribution of Vglut2 (black dots), retrograde (blue dots) and double-labeled (red dots) cells in the forebrain following Fluoro-Gold injections into the medial prefrontal cortex are shown in a series of rostro-caudal sections (Case 35). **A:** Double-labeled cells are abundant in the claustrum. **B:** Vglut2 projection neurons are scattered among the single retrograde neurons in the MS/VDB, rostral substantia innominata (SI), and ventral pallidum (VP). **C:** Several double-labeled cells are distributed within the lateral and medial preoptic areas (LPO, MPA) and VP. **D:** Despite abundant retrograde labeling in basal forebrain areas, only a minor proportion of these cells contain Vglut2. Double labeling is found in the MPA, lateral hypothalamic area (LH), SI, and HDB. Scale bar = 1 mm.

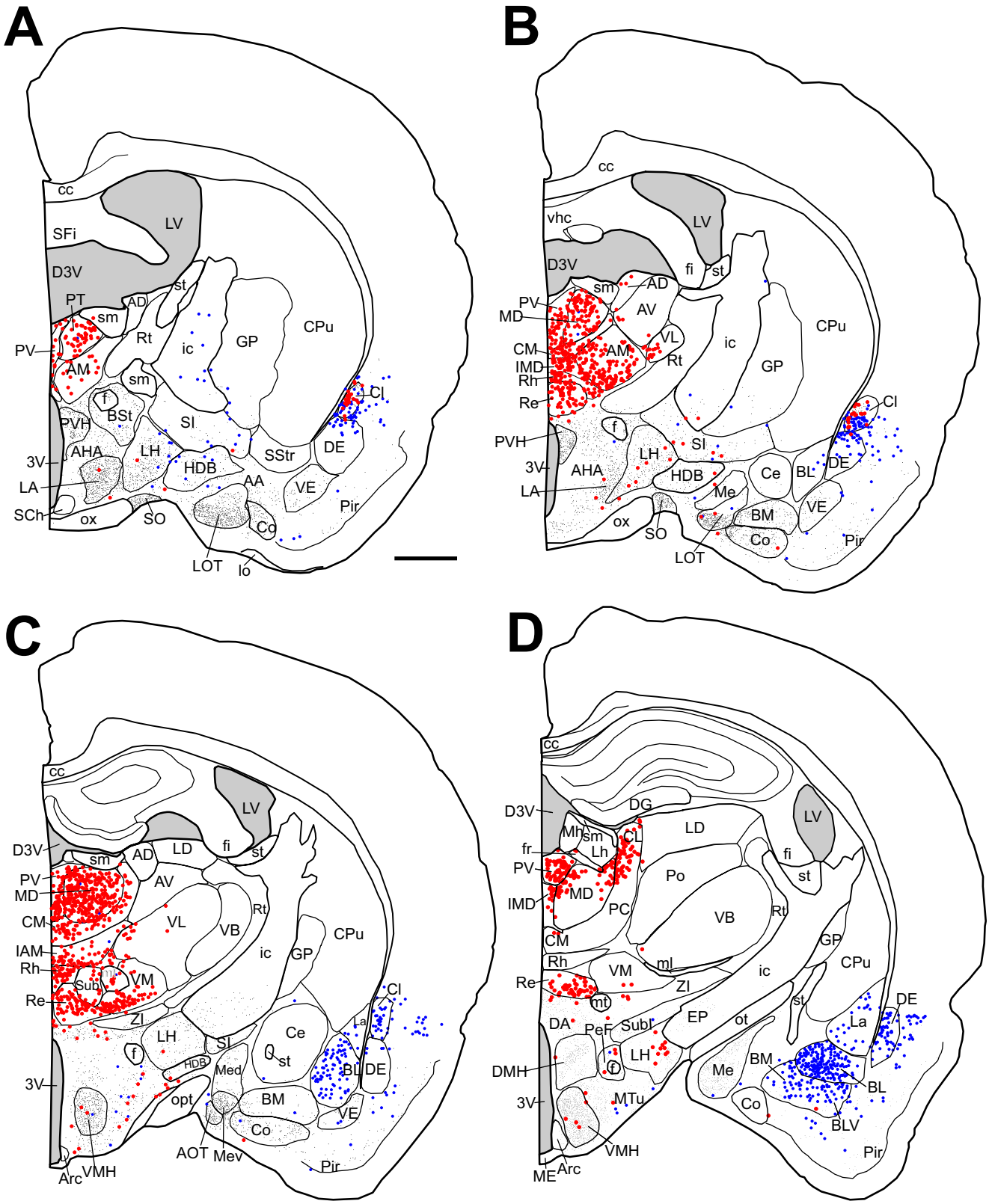

Fig. 5. Distribution of Vglut2 (black dots), retrograde (blue dots), and double-labeled (red dots) cells in the forebrain after injection of Fluoro-Gold into the medial prefrontal cortex shown in a series of coronal maps caudal to Figure 4 (Case 35). Note the abundance of double-labeling in the midline, intralaminar, and medial thalamic nuclei and the claustrum. **A:** Scattered double-labeled cells appear in the lateral anterior hypothalamic nucleus (LA) and lateral hypothalamic area (LH). **B:** Several double-labeled cells are distributed diagonally across the lateral hypothalamic area (LH). Basal forebrain areas, including the HDB, substantia innominata (SI), and internal capsule contain a few double-labeled cells. **C:** Double labeling is absent in the lateral (La), basolateral (BL), and basomedial (BM) amygdaloid nuclei, although these areas are rich in retrogradely labeled cells. **D:** The lateral hypothalamic area (LH), the posterior hypothalamic area (PH), the perifornical area (PeF), and the medial tuberal nucleus (MTu) contain several double-labeled cells. Scale bar = 1 mm.

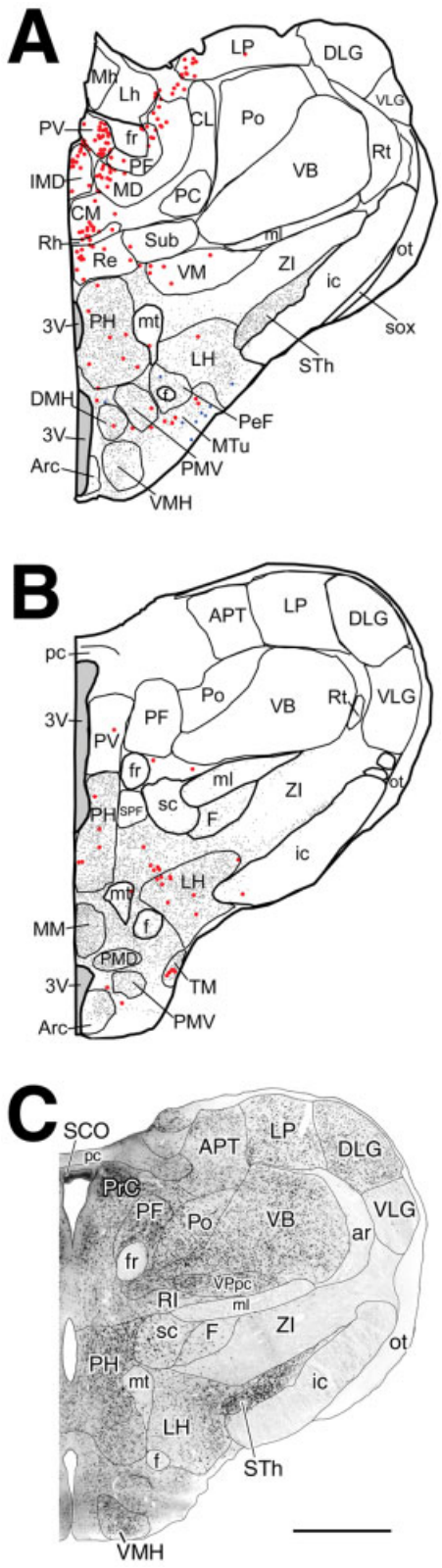

hypothalamus (3.8%), brainstem (0.7%), amygdala (0.5%), basal forebrain (0.4%), and piriform cortex (0.2%). The estimated total number of double labeled cells is given in Table 2.

Basal forebrain. Very few retrogradely labeled cells are dispersed in the dorsal and middle parts of MS/VDB (Fig. 4A–C). On the other hand, large numbers of retrogradely labeled cells are visible in the ventrolateral part of the VDB towards the transition to the HDB. This group of retrogradely labeled cells blends with labeled cells within the area between the MS/VDB and ventral pallidum and seems to correspond to the rostral part of the substantia innominata (Fig. 4B). Within the ventral pallidum, there are many retrogradely labeled cells, mainly in the middle of its mediolateral extent (Fig. 4B). Behind the crossing of the anterior commissure, retrogradely labeled cells heavily populate the medial part of globus pallidus at its border towards the internal capsule, substantia innominata, and mediodorsal part of HDB. The HDB contains scattered retrogradely labeled cells all along its rostrocaudal extent. Very few retrogradely labeled cells are visible in the bed nucleus of the stria terminalis (Figs. 4D, 5A). The substantia innominata contained a few retrogradely labeled cells caudally, as shown in Figures 4D, 5A,B. From three brains, out of 696 retrogradely labeled cells in the entire basal forebrain only 35 were double-labeled (5%). A double-labeled cell in the HDB can be seen among several retrogradely labeled cells in Figure 8A–C.

Hypothalamus and preoptic area. Retrogradely labeled cells are diffusely distributed in the hypothalamus, including the lateral hypothalamus, posterior hypothalamic area, and perifornical area. Retrogradely labeled cells are abundant in the area termed tuber cinereum by Paxinos and Watson (1998), including the ventromedial hypothalamic nucleus (Fig. 5C,D). Despite the diffuse nature of the retrograde cells, it is apparent that labeled cells are organized into sheets traversing the anterior-lateral hypothalamic areas towards the substantia innominata and internal capsule (Fig. 5B–D). Fewer double-labeled cells are located in other hypothalamic regions, including the dorsomedial (Fig. 5D) and lateroanterior hypothalamic nuclei (Fig. 5A,B), and medial and lateral preoptic areas (Fig. 4C,D). Out of 879 retrogradely labeled hypothalamic cells in three brains, 311 (35%) also contained Vglut2.

Claustrum, piriform cortex, and amygdala. About 32% of all retrogradely labeled cells in the claustrum that projected to the mPFC contained Vglut2. Several examples of double-labeled cells in the claustrum can be seen in

Fig. 6. Distribution of Vglut2 (black dots), retrograde (blue dots), and double-labeled (red dots) cells in the forebrain after injection of Fluoro-Gold into the medial prefrontal cortex caudal to Figure 5 (Case 35). **A:** The bulk of the double labeling occurs within several midline-intralaminar thalamic nuclei. There is also some double labeling in the medial part of ventromedial and lateroposterior thalamic nuclei. Double labeling is found mostly in the posterior and lateral hypothalamic areas (PH, LH), medial tuberal nucleus (MTu), and perifornical area (PeF). Occasional double labeling can be seen in the dorsomedial hypothalamic nucleus (DMH) and the ventral premammillary nucleus (PMV). **B:** Double labeling occurs in the LH, PH, and tuberomammillary nucleus (TM). **C:** Widespread Vglut2 expression is shown in a digital photomontage at the level of the posterior hypothalamus for comparison with A and B. Bregma –3.8 mm. Scale bar = 1 mm.

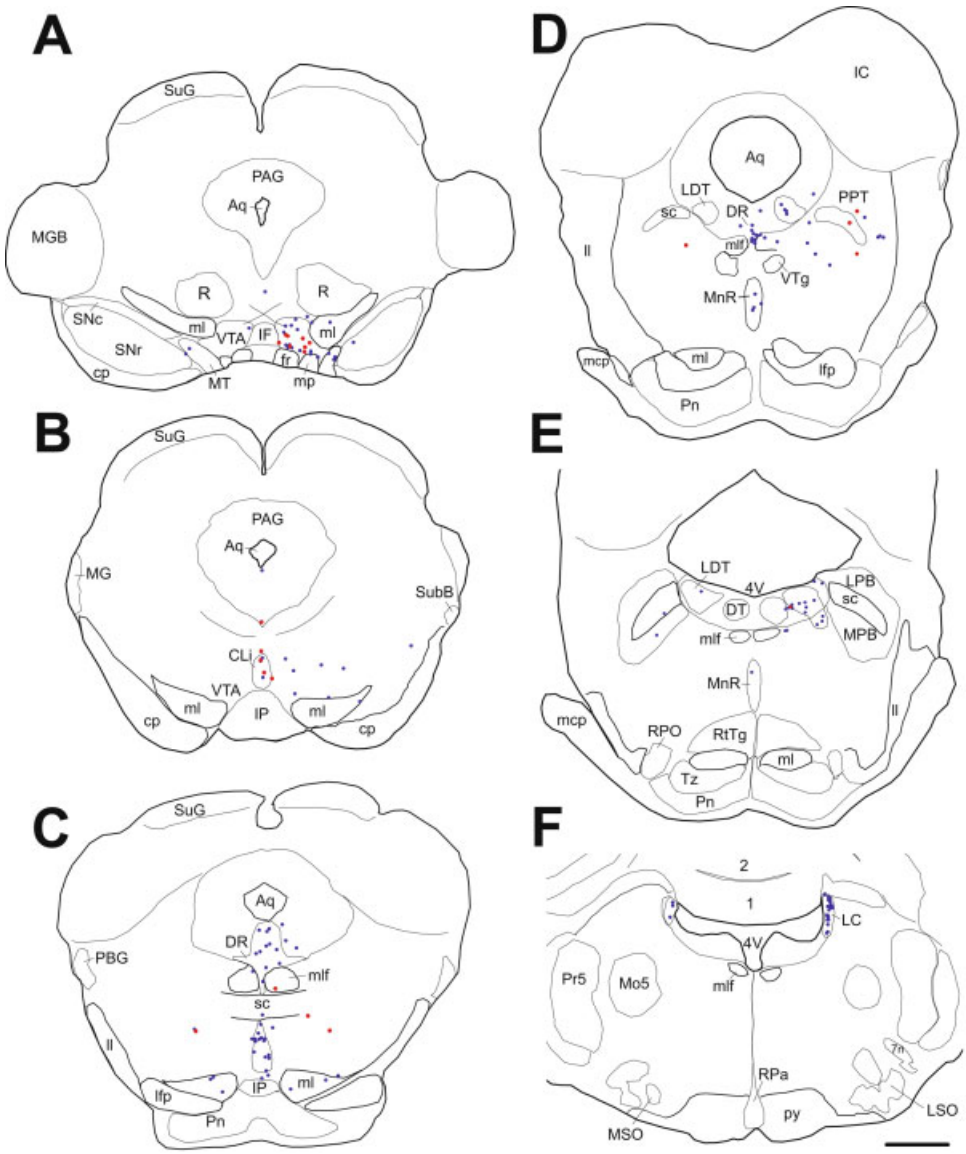

Fig. 7. Distribution of single retrograde (blue dots) and double-labeled cells (red dots) in the brainstem following Fluoro-Gold injection into the medial prefrontal cortex (Case 35). The largest amount of double-labeling in the brainstem is found in the ventral tegmental area (VTA). There is also double labeling in the caudal linear raphe nucleus (CLi), and laterodorsal (LDT) and pedunculopontine tegmental (PPT) nuclei. Single retrogradely labeled cells are located within the locus coeruleus (LC), and several raphe nuclei. Scale bar = 1 mm.

Figure 8D–F. The piriform cortex, including the dorsal and ventral endopiriform regions, contained 6,391 retrogradely labeled cells. From three brains, 13 cells were double-labeled (<1%). In the amygdala 3,044 retrogradely labeled cells were mapped from three brains, but only 41 of them were double-labeled (1.3%).

Thalamus. The midline/intralaminar (paraventricular, paratenial, reuniens, rhomboid, centromedial, centrolateral, and intermediodorsal), and medial "association" thalamic nuclei (mediodorsal, anteromedial, interanteromedial) contained massive retrograde labeling. For classification of thalamic nuclei, refer to Price (1995) and Faull and Carman (1978) for the ventral thalamic nuclei. Almost 100% of the thalamic retrogradely labeled cells also expressed Vglut2 mRNA (Figs. 5, 6A; Table 3). Figure 9A–C shows large numbers of double-labeled cells at the border between the mediodorsal and paraventricular thalamic nuclei.

Brainstem. Retrogradely labeled cells were found in the ventral tegmental area, raphe nuclei (dorsal, median, caudal linear), the locus coeruleus, and the laterodorsal and pedunculopontine tegmental nuclei. From a total of 425 retrogradely cells in the brainstems of two animals, 60 neurons were double-labeled (14%). The majority of double-labeled cells were scattered outside the traditional border of the above-mentioned brainstem nuclei. From the 37 double-labeled neurons in Case 35, there were eight neurons in the ventral tegmental area and four in the caudal linear nucleus (Table 5). Figure 9D–F shows double-labeled cells in the ventral tegmental area.

Distribution of retrograde and double-labeled cells following primary somatosensory cortical injections

Injections sites and cell numbers. Tracer injections into S1 were analyzed in Cases 01, 34, and 68. The injections were located in different rostrocaudal parts of S1 (Fig. 3). In Cases 34 and 68, the injections were centered in the medial part of the sensory jaw region, with an

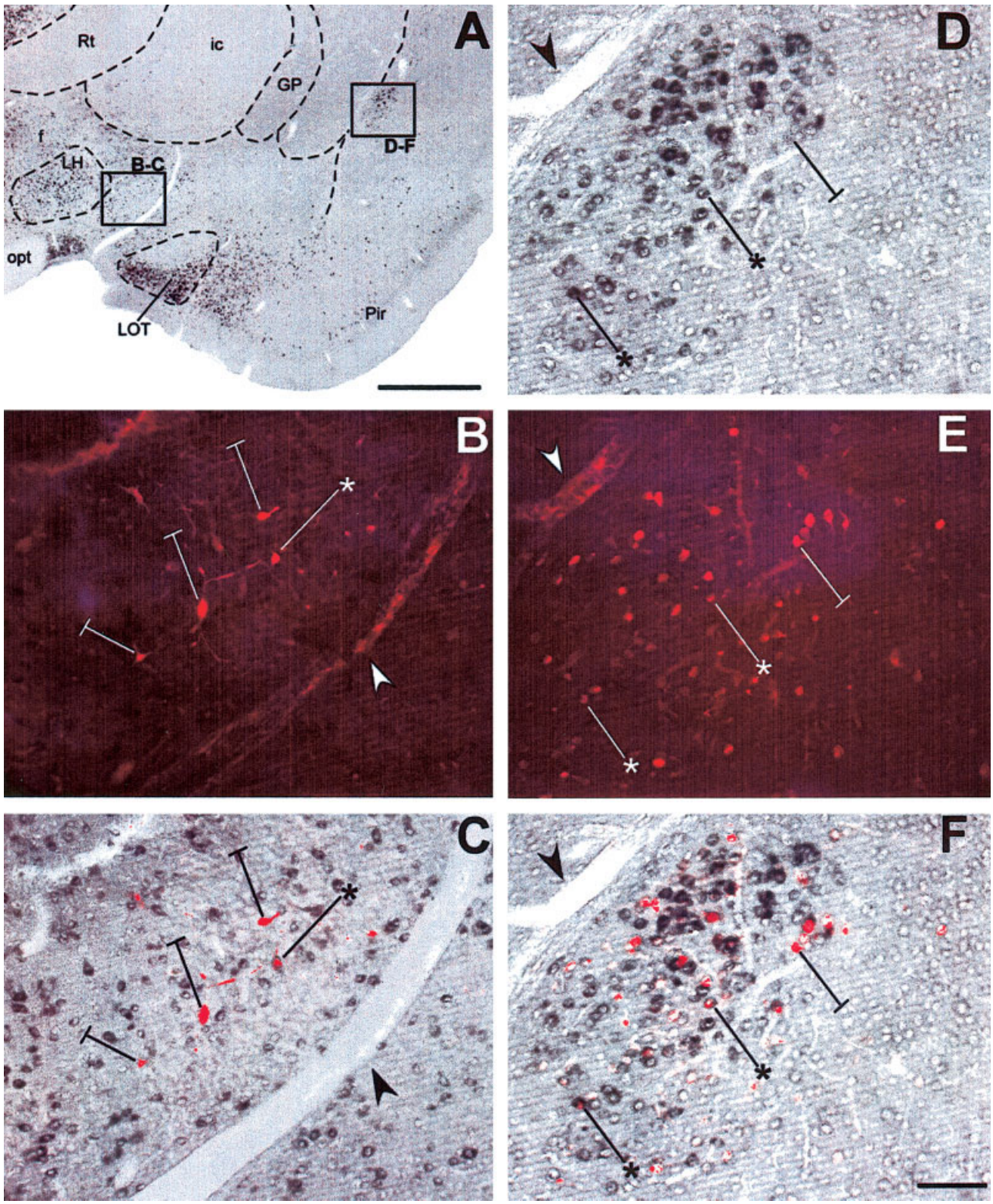

Fig. 8. Digital photomicrographs of Vglut2 and retrogradely labeled cells in the caudal part of the horizontal limb of the diagonal band (HDB) and claustrum (Cl) following Fluoro-Gold injection into the medial prefrontal cortex (Case 35). **A:** Low-magnification photomicrograph of a forebrain section at about 1.4 mm behind bregma. The boxes in the HDB and Cl indicate the location of cells in panels B,C and D–F, respectively. **B:** retrograde labeling revealed by a Cy3 tag for Fluoro-Gold. **C:** A superimposed image of Vglut2 and Cy3 labeling (from B) reveals a double-labeled cell (asterisk). Flat-headed arrows point to retrogradely labeled cells that are not positive for Vglut2. **D:** Vglut2 expression is abundant in the claustrum. **E:** Retrogradely labeled cells in the claustrum. **F:** Superimposed image of Vglut2 expression (D) and retrogradely labeled cells (E) shows several double labeled cells in the claustrum. Scale bar = 500 μm in A; 50 μm in B (applies to B–F).

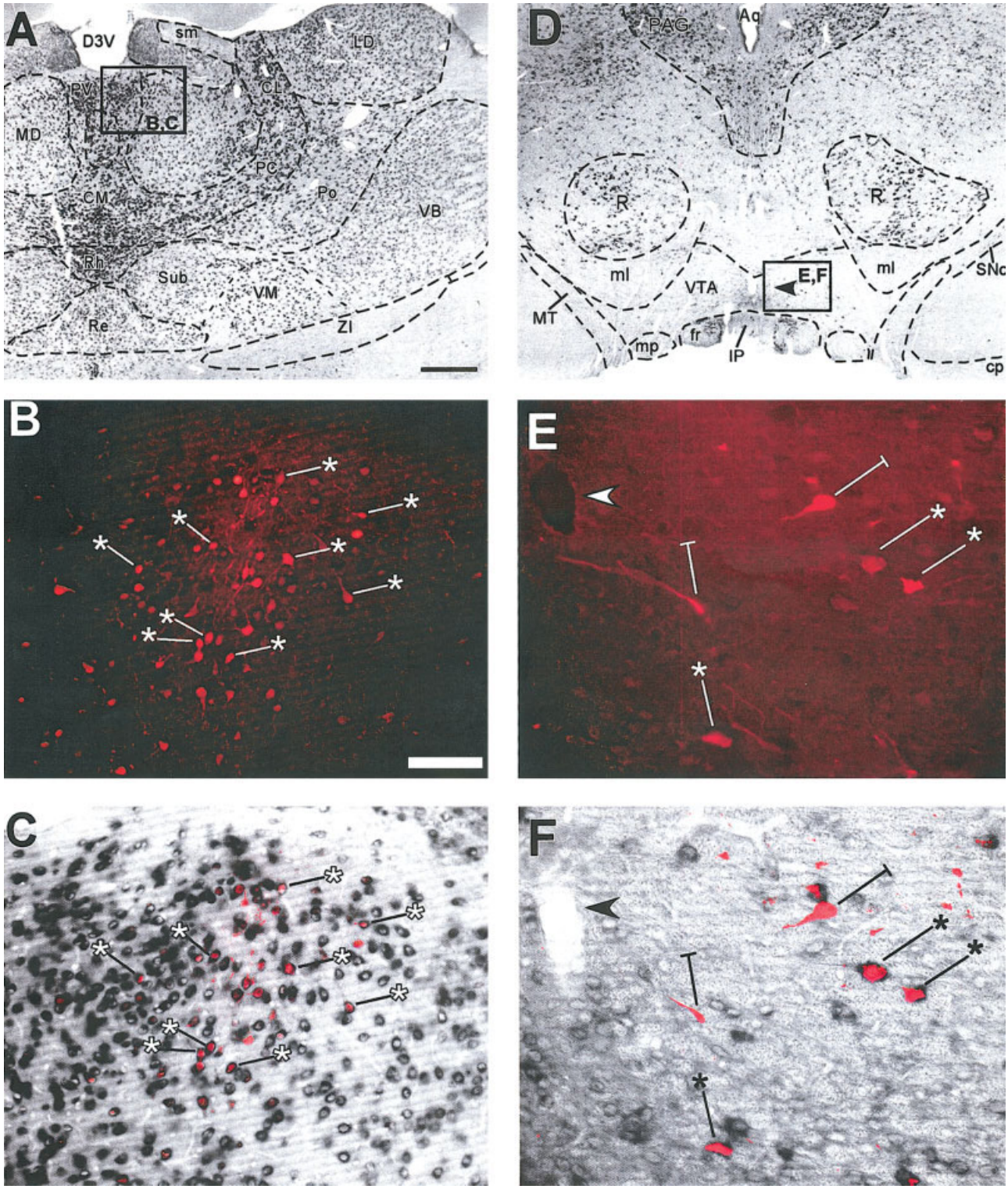

Fig. 9. Thalamocortical projection neurons from the paraventricular and mediodorsal thalamic nuclei contain Vglut2 mRNA (Case 35). Several cells, marked with asterisks, were chosen as examples of double labeling (B,C). **A:** Low-magnification digital micrograph of the thalamus. Although Vglut2 labeling is apparent in all nuclei shown, the darkest labeling is found in the midline (periventricular, rhomboid nuclei) and intralaminar (centromedial, paracentral, centrolateral) nuclei. The area of the box is magnified in B,C. **B:** Many cells along the border between the mediodorsal (MD) and paraventricular (PV) thalamic nuclei contain Vglut2. **C:** A digital micrograph of the same field under red fluorescence shows retrograde labeling along the border of the periventricular and mediodorsal thalamic nuclei (in B). Superimposed image of Vglut2 and FG-Cy3 fluorescence reveals that the majority of retrogradely labeled neurons is positive for Vglut2 mRNA. **D:** A low-magnification digital photomicrograph of Vglut2 labeling in the midbrain. The periaqueductal gray (PAG), red nucleus (R), and the ventral tegmental area (VTA) contain Vglut2 mRNA. An arrowhead marks a capillary used as a fiducial marker. **E:** FG-Cy3 demonstrates retrograde neurons in the VTA. **F:** In the superimposed brightfield and fluorescent image of the same field as E, double-labeled cells are marked with asterisks. Single retrogradely labeled neurons are indicated with flat-headed arrows. Scale bar = 500 μm in A (applies to A,D); 50 μm in B (applies to B,C,E,F).

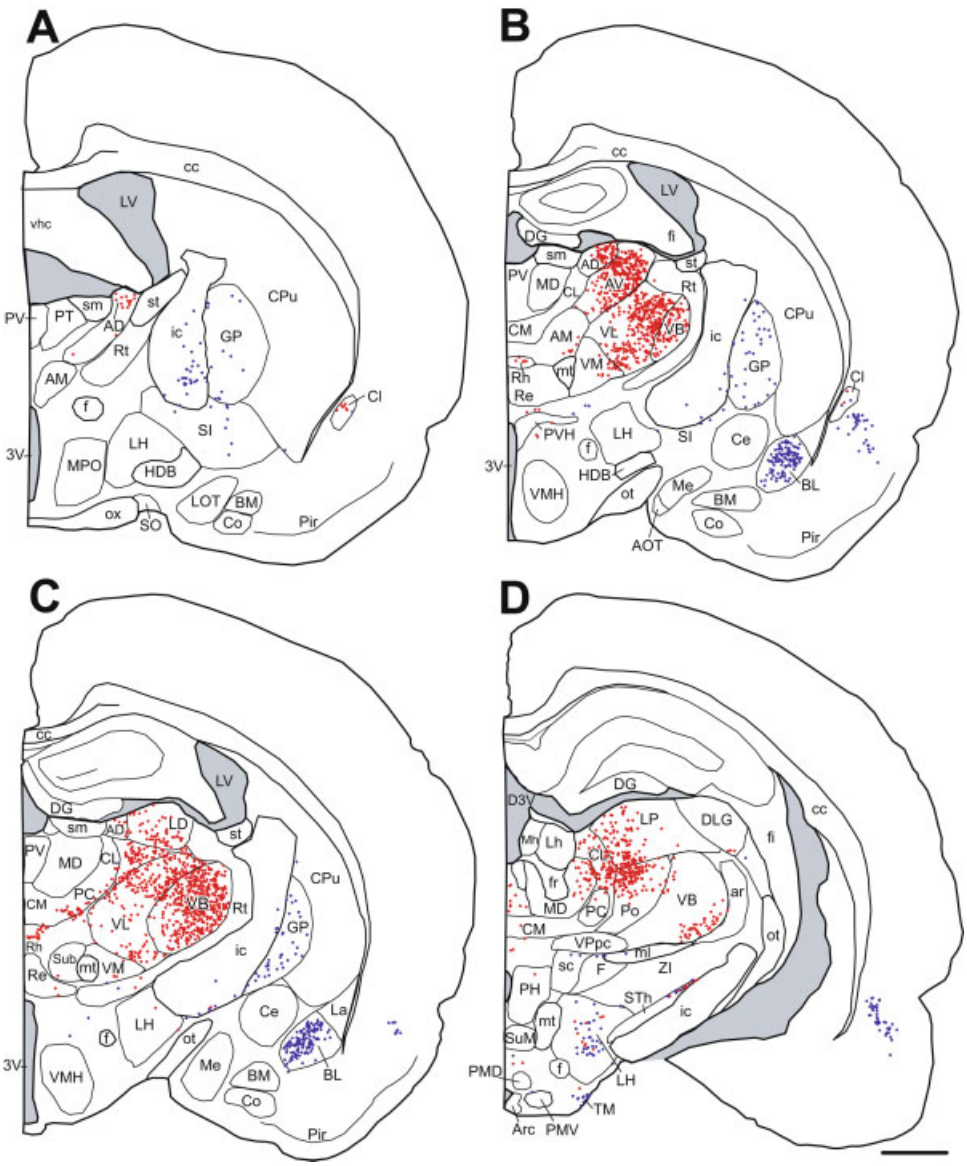

Fig. 10. Distribution of single retrograde and double-labeled cells (Vglut2 and Fluoro-Gold) in the forebrain after injection of the tracer in the somatosensory cortex shown in four rostrocaudal (**A–D**) coronal maps of Case 01. Red dots represent double-labeled cells; blue dots symbolize single Fluoro-Gold-labeled cells. The majority of double-labeled cells are in the relay thalamic nuclei, including the ventrobasal (VB), ventrolateral (VL), anterior (AD, AV), dorsal (LD, LP). Several intralaminar nuclei (PC, CL, Rh) contain scattered double-labeled cells. In the hypothalamus the lateral hypothalamic area (LH) at posterior tuberal level contain several retrograde and double-labeled cells (D). The claustrum contains moderate amount of double-labeled cells. The basolateral amygdaloid nucleus (BL) is heavily labeled by retrograde cells; however, none contain Vglut2. Basal forebrain areas, including the substantia innominata (SI), globus pallidus (GP), and internal capsule (ic) contain single retrogradely labeled neurons and no double-labeling. Scale bar = 1 mm.

encroachment of the lateral part of the primary motor cortex. In Case 68, the forelimb cortical area was injected. Finally, in Case 01, in addition to forelimb, the dysgranular zone, upper lip, and the medial barrel field were labeled. Fifty-three percent of all (n = 12,984) cells projecting to S1 were double-labeled. The thalamus accounted for about 96% of the double-labeled cells (Table 4). The remaining portion comes from claustrum (2.9%), basal forebrain (0.4%), hypothalamus (0.3%), brainstem (0.3%), and amygdala (0.1%).

Figure 10 displays four mapped coronal sections from Case 01. Few retrogradely labeled cells were encountered also in the basal forebrain areas (MS/VDB, HDB, and ventral pallidum) but none of them were double-labeled (not shown). There were many retrogradely labeled cells in the globus pallidus and internal capsule, and in the neighboring substantia innominata, a few cells were double-labeled (4%). The amygdala had only eight double-labeled cells out of 4,660 total retrogradely labeled cells from three brains. The brainstem contained about 80 retrogradely labeled cells with a small proportion double-labeled (9%) in the ventral tegmental area and the posterior intralaminar nuclei (Fig. 11A). Ninety-nine percent of the thalamic retrogradely labeled neurons also expressed Vglut2 (Table 4). These labeled cells were distributed primarily in the ventrobasal, ventral anterior, anteroventral, lateroposterior, and laterodorsal thalamic nuclei. A few labeled cells were also observed in the intralaminar (centrolateral, paracentral) thalamic nuclei and in the lateral part of the mediodorsal thalamic nucleus (Table 6).

Comparison of prefrontal and somatosensory cases

Adjusting for injection volume (1.0×10^7 μm^3), the number of retrogradely labeled cells was significantly larger in brains with prefrontal cortex injections (one-

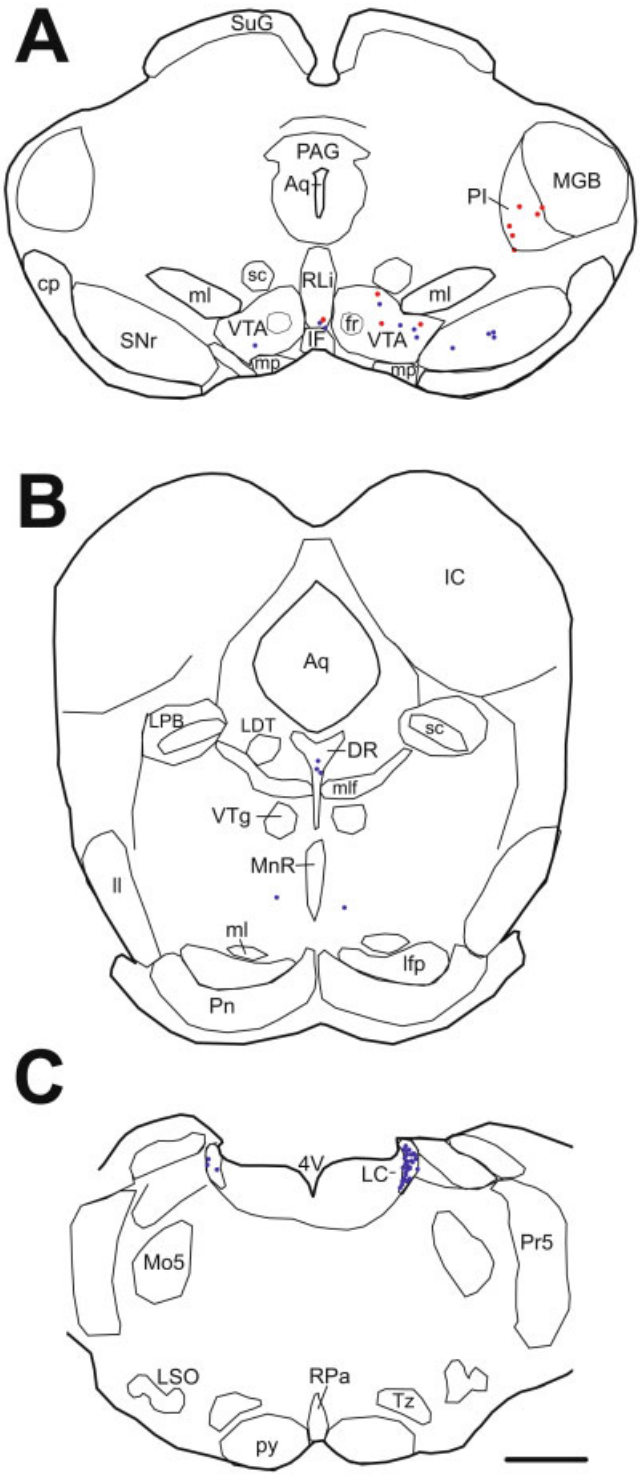

Fig. 11. Distribution of retrogradely and double-labeled cells in the brainstem after FluoroGold injection in the somatosensory cortex shown on three coronal sections of Case 34 (**A–C**). Most of the double-labeled neurons are located in ventral tegmental area (VTA), and in the posterior intralaminar complex (PI). Scattered double-labeled cells were noted also in the rostral linear nucleus of the raphe (RLi). The locus coeruleus (LC) contains numerous retrogradely labeled cells without Vglut2 expression. Scale bar = 1 mm.

tailed t-test, $t(2.00067) = 3.22$, $P < 0.045$) than in cases with somatosensory injections. The number of double-labeled cells per 1.0×10^7 μm^3 injection volume was also significantly larger in prefrontal injections than for primary somatosensory injections (one-sided t-test, $t(2.024) = 4.68$, $P < 0.025$). The number of double-labeled cells in the hypothalamus in the prefrontal cases was significantly higher than for the somatosensory injection cases (one-sided t-test, $t(4.0) = 2.26$, $P < 0.04$).

DISCUSSION

This is the first systematic study of the distribution of Vglut2 neurons in the forebrain using in situ hybridization. From combined retrograde tracer injections and in situ hybridization, the thalamus was found to supply the majority of Vglut2 input to mPFC and S1, i.e., 90% to the prefrontal and 96% to somatosensory cortices. Vglut2 contributions to these cortical areas also originated from the hypothalamus-basal forebrain, claustrum, and the brainstem. The present data suggest that the prefrontal cortex receives significantly more Vglut2 input than somatosensory cortex from subcortical areas. The percentage distribution from subcortical areas also varies according to their neocortical target. For example, hypothalamic Vglut2 cells projecting to the prefrontal cortex constitute a higher percentage of the extrathalamic Vglut2 input than those projecting to the somatosensory cortex.

Technical considerations

Specificity. Due to the high sequence homology of Vglut1 and Vglut2 (Bai et al., 2001; Fremeau et al., 2001; Herzog et al., 2001) it was important to choose a probe sequence that binds uniquely to the Vglut2 transporter mRNA. Our riboprobes were constructed from the portion of the gene encoding the unique C-terminus of Vglut2 protein (Stornetta et al., 2002). However, a probe that is too long may be able to hybridize with portions of complementary sequences from other proteins, creating nonspecific labeling. The necessary controls for in situ hybridization are probes with the sense sequence and probe sequencing. Our sense controls for Vglut2 had minimal to no labeling (not shown).

Digoxigenin probe. We developed the Vglut2 digoxigenin cRNA probes to be processed by colorimetric detection. The alkaline phosphatase reaction is necessary for the visualization product of in situ hybridization, but overincubation of the sections during the alkaline phosphate reaction will produce precipitate in nonglutamatergic neurons as well. However, the intensity of the reaction product also depends on the amount of mRNA present in the cell. Thus, the darkest Vglut2 staining regions such as the thalamus are, indeed, highly glutamatergic. In contrast, the reticular thalamic nucleus is devoid of Vglut2 staining. The termination of the alkaline phosphatase reaction was determined by the amount of time needed to label reticular thalamic nuclei (nonspecific staining). The completed reactions were between 3–4 hours and Vglut2 cells were darkly labeled against a lighter background.

Combination with retrograde tracer. Either floating sections or slide-mounted sections can be used for in situ hybridization. We chose to use free-floating sections for the numerous washing steps in the in situ hybridization protocol and subsequent immunocytochemical incubations. However, we and others (Stornetta et al., 2002) have

observed that excessive rinsing needed for in situ hybridization attenuates the Fluoro-Gold (FG) signal. As a result, much of the original FG fluorescence is lost, although a faint FG labeling can still be detected. To remedy this, during incubation of digoxigenin antibody we also added a primary antibody against FG. By performing immunocytochemistry concurrently with in situ hybridization, we reduced the probability of losing the FG signal at the end of the hybridization procedure. Comparing the number of in situ hybridization-fluorescent cells (anti-FG developed with Cy3) to an FG series mounted from the same brain without in situ hybridization, in five of the six brains there was no difference in the location or quantity of retrogradely labeled cells. However, there was a 50% loss of retrograde cells following in situ hybridization in one case. In this regard, we may be underestimating the actual number of retrograde and double-labeled cells.

Distribution of Vglut2 cells

In agreement with previous studies of the hypothalamus, the ventromedial nucleus is heavily labeled for Vglut2 mRNA (Hisano et al., 2000; Ziegler et al., 2002; Lin et al., 2003). However, there are discrepancies in density grading for the same nucleus (e.g., compare ventromedial and premammillary nuclei in the respective articles). Although two groups (Hisano et al., 2000; Ziegler et al., 2002) used the same length of Vglut2 riboprobes (700 bp) and the third group (Lin et al., 2003) used a shorter riboprobe, it is expected that the relative labeling intensity would be comparable. The discrepancy in their reported densities can be explained in part by the usage of qualitative, descriptive terms. For example, it is unclear whether only grains/cell are evaluated (Ziegler et al., 2002) or cell numbers are also considered (Hisano et al., 2000; Lin et al., 2003).

So far only one study (Lin et al., 2003) compared immunostaining with in situ hybridization for the expression of Vglut2 cells. For the immunocytochemical localization of Vglut2 in cell bodies, Lin et al. (2003) used colchicine. In some cases, like the lateral hypothalamic area, the protein is apparently expressed in fewer cells than those developed for mRNA, while in the supraoptic nucleus the opposite is true. Due to the subjective grading of mRNA values, and the uncertainty whether the intensity or the cell number is reported in this article, further systematic studies are necessary to determine to what extent mRNA will be translated to protein in the individual brain regions.

In our study, the number of cells were counted and adjusted per unit tissue volume. In this way, the cell densities of various brain regions can be compared. However, for a functional interpretation the absolute number of labeled cells within a given structure has to be taken into account (Table 2).

It is interesting to note that the Vglut2 cell density shows striking differences across brain regions, yet cell groups with similar density seem to be anatomically and functionally interrelated. For example, the amygdaloid nuclei (nucleus of the lateral olfactory tract, medial, and cortical amygdaloid nuclei) and the ventromedial hypothalamic nucleus that participate in the accessory olfactory circuitry (Shipley et al., 1995) have the highest Vglut2 cell densities in the rat forebrain. Similarly, basal forebrain structures, including MS/VDB, HDB, substantia innominata, pallidal areas, and the internal capsule contain a moderate-to-low Vglut2 cell density. Future studies are needed to determine if, indeed, developmentally and hodologically related structures show similar expression of the various isotypes of vesicular glutamate transporters.

Corticopetal projections

Lorente de No (1938) gave the first systematic description of corticopetal projections with two types of fibers entering the cerebral cortex: one that terminates primarily in Layers III and IV of a restricted area of the cortex termed "specific," and another that gives rise to multiple, radially oriented collaterals innervating Layers I and VI over wide areas in the cortex ("nonspecific" or diffuse). He suggested that the specific fibers originated in the sensory thalamic nuclei mediating visual, auditory, and somatosensory information, while the nonspecific fibers arose from the midline and intralaminar thalamic nuclei. Anatomical studies in subsequent years established that, in addition to the intralaminar thalamic nuclei, the nonspecific afferents to the cortex originate from several brainstem and forebrain regions. Together, these afferents represent the diffuse extrathalamic corticopetal systems (Saper, 1987). However, individual midline and intralaminar nuclei receive distinct sets of inputs and project to restricted areas of the neocortex (Groenewegen and Berendse, 1994; Jones, 1998; Van der Werf et al., 2002). Additionally, mounting physiological evidence in rat and monkey support the idea that individual intralaminar nuclei participate in a diversity of functions such that even the "diffuse" system is specifically organized as well (for review, see Groenewegen and Berendse, 1994; Van der Werf et al., 2002).

Thalamocortical projection. Our data demonstrate that the mPFC receives thalamic projections from midline, intralaminar, and association relay nuclei, whereas thalamic afferents to primary somatosensory cortex arise principally from the ventrobasal nucleus, posterior nuclear groups, and intralaminar nuclei. These data are consistent with the literature, such that the mPFC receive thalamic projections from mostly medially located nuclei and the somatosensory cortex primarily from lateral thalamic nuclei, observing a close-to-sagittal topography across nuclear borders in primates (Kievit and Kuypers, 1977) and rodents (Jones and Leavitt, 1974; Herkenham, 1979, 1986; Donoghue and Parham, 1983; Thompson and Robertson, 1987; Groenewegen, 1988; Berendse and Groenewegen, 1991; Fabri and Burton, 1991; Van Groen and Wyss, 1992; Price, 1995; Reep et al., 1996; Reep and Corwin, 1999; Jones, 2001; Van der Werf et al., 2002).

The presence of labeled cells following somatosensory cortex injection (Cases 01 and 68) in the laterodorsal and lateroposterior nuclei are likely due to the encroachment of the injection site on the posterior parietal cortex which receives projections from these nuclei but not from the ventrobasal complex (Sanderson et al., 1991; Reep et al., 1994). Additionally, labeled cells in the laterodorsal and lateroposterior nuclei may originate from the adjacent lateral part of the primary motor cortex that overlaps partially with the sensory hindpaw and forepaw regions (Jones and Leavitt, 1974; Donoghue et al., 1979; Reep et al., 1994; Price, 1995; Reep and Corwin, 1999). Also, axons from the laterodorsal and lateroposterior nuclei en route to the cingulate and retrosplenial cortices might have taken up the tracer (Thompson and Robertson, 1987; Van Groen et al., 1992).

About 99% of the retrogradely labeled cells in the thalamus were colocalized with Vglut2, confirming physiological evidence that thalamocortical fibers use glutamate as their transmitter (Steriade et al., 1997). Although the total numbers of thalamic cells labeled from prefrontal and somatosensory cases are comparable (see Thalamus in Tables 3 and 4), labeling in relay vs. midline-intralaminar nuclei is different. As the data from Table 6 suggest, the Vglut2 thalamic input to the mPFC from the association relay nuclei is slightly larger that the portion originating from midline-intralaminar nuclei. However, the Vglut2 thalamic projection to the somatosensory cortex originating in the sensory and motor relay nuclei exceeds the number of projection neurons in midline-intralaminar nuclei by several factors. If the proportion of glutamatergic contribution from the relay nuclei will be proven to be higher than those from the intralaminar nuclei in other sensory modalities, this would suggest that the intralaminar-midline nuclei play a more important role in modulating prefrontal than sensory cortical functions.

Extrathalamic corticopetal projection

Monoaminergic systems. Since the original description of brainstem monoaminergic cell groups by Dahlström and Fuxe (1964), numerous studies confirmed the presence of corticopetal projections from the noradrenergic locus coeruleus (Aston-Jones et al., 1995), serotoninergic raphe (Kosofsky and Molliver, 1987), and dopaminergic midbrain nuclei (Fallon and Loughlin, 1995). According to our study, both the prefrontal and somatosensory cortices received abundant projections from the ventral tegmental area, various raphe nuclei, and the locus coeruleus. Ten to twenty percent of all retrograde cells in the brainstem were found to express Vglut2. The presence of N-acetyl-aspartyl-glutamate, which can be hydrolyzed to produce glutamate into synaptic clefts, has been described earlier in serotoninergic neurons (Forloni et al., 1987). However, most likely Vglut3 is the transporter for glutamate in the raphe (Gras et al., 2002; Schafer et al., 2002). In agreement with Stornetta et al. (2002), Vglut2 was not found in the locus coeruleus. However, some cultured substantia nigra dopaminergic neurons have been shown to be colocalized with Vglut2 (Dal Bo et al., 2004).

Pontocortical projection system. According to our data, a small proportion of mesopontine Vglut2 cells project to the prefrontal cortex, in agreement with earlier studies showing that the laterodorsal tegmental nucleus innervates this cortical region (Satoh and Fibiger, 1986). The projection from the laterodorsal tegmental nucleus has been shown in part to contain acetylcholine (Satoh and Fibiger, 1986). Since glutamatergic neurons in the mesopontine tegmentum are intermingled or colocalized with cholinergic neurons (Clements and Grant, 1990) and a dual cholinergic and glutamatergic input from this region projects to the substantia nigra (Lavoie and Parent, 1994), it is possible that the mesopontine Vglut2 projection to the prefrontal cortex also contains acetylcholine.

Hypothalamocortical projections. Our study confirmed that neurons in the hypothalamus project according to a mediolateral topography to medial prefrontal and somatosensory cortices (Saper, 1985). For example, neurons targeting the somatosensory cortex were more laterally located than those projecting to the mPFC. In our study, about 39% of the extrathalamic glutamatergic neurons projecting to the mPFC originates from the hypothalamus. On the other hand, only 7% of the Vglut2-expressing extrathalamic neurons projecting to S1 originated from the hypothalamus. Some of these neurons may contain histamine (Takeda et al., 1984), hypocretin/orexin (Peyron et al., 1998), or melanin-concentrating hormone (Broberger et al., 1998). According to a recent study, up to 50% of orexin-positive cells also contain Vglut2 (Rosin et al., 2003). However, it is unclear whether or not the orexin/Vglut2 cells actually project to the neocortex, since orexin2-receptor-expressing cells in the cerebral cortex are localized primarily in Layer VI (Marcus et al., 2001), a layer that contains few Vglut2 terminals (Kaneko et al., 2002).

Projections from basal forebrain regions. There are several lines of evidence that the basal forebrain is involved in controlling cortical activity through widespread projections to the cortex and hippocampus (Saper, 1984; Detari and Vanderwolf, 1987; Buzsaki et al., 1988; Duque et al., 2000; Manns et al., 2000; Zaborszky and Duque, 2003). In rat, cholinergic cells make up only about half of the neurons projecting to the prefrontal and somatosensory areas; the rest are GABAergic or peptidergic (Gritti et al., 1997; Zaborszky et al., 1999; Zaborszky and Duque, 2003). A glutamatergic projection from the basal forebrain to the cortex has been suggested, based on basal forebrain stimulations (Jimenez-Capdeville et al., 1997). Using Vglut2 as the definitive marker of glutamatergic neurons, we found only 5% of retrogradely labeled cells in the basal forebrain expressing Vglut2. This is in contrast to a study by Manns et al. (2001) that reported 80% of basal forebrain cells projecting to the entorhinal cortex were interpreted to be glutamatergic using phosphate-activated glutaminase immunoreactivity. Although phosphate-activated glutaminase has been used in the past for labeling putative glutamatergic neurons, other studies have shown that phosphate-activated glutaminase is also present in GABAergic neurons (Kaneko and Mizuno, 1988; Akiyama et al., 1990; Kaneko et al., 1992; Laake et al., 1999), indicating that this enzyme is not specific for glutamatergic neurons.

Transmitter glutamate within cholinergic basal forebrain cells has been suggested by the colocalization of N-acetyl-aspartyl-glutamate in cholinergic MS/VDB neurons (Forloni et al., 1987). Glutamate is released in addition to acetylcholine from isolated cholinergic cortical synaptosomes, indicating that glutamate might also be released from cholinergic terminals in the cerebral cortex (Docherty et al., 1987). However, a reinvestigation suggested that only a minor proportion of cholinergic cells may be glutamatergic (Szerb and Fine, 1990). Glutamatergic basal forebrain neurons may have a role in the synaptic modulation of corticopetal basal forebrain neurons, as it has been shown that parvalbumin-containing septohippocampal neurons receive input from local Vglut2 neurons (Hajszan et al., 2004).

It is interesting to note that the mPFC receives a smaller amount of cholinergic input than the somatosensory cortex (Gritti et al., 1997), while our study suggests that the opposite is true for Vglut2 input to these two cortical areas. Morphological and electrophysiological studies suggest that cholinergic terminals in these two cortical areas may interact with glutamatergic terminals

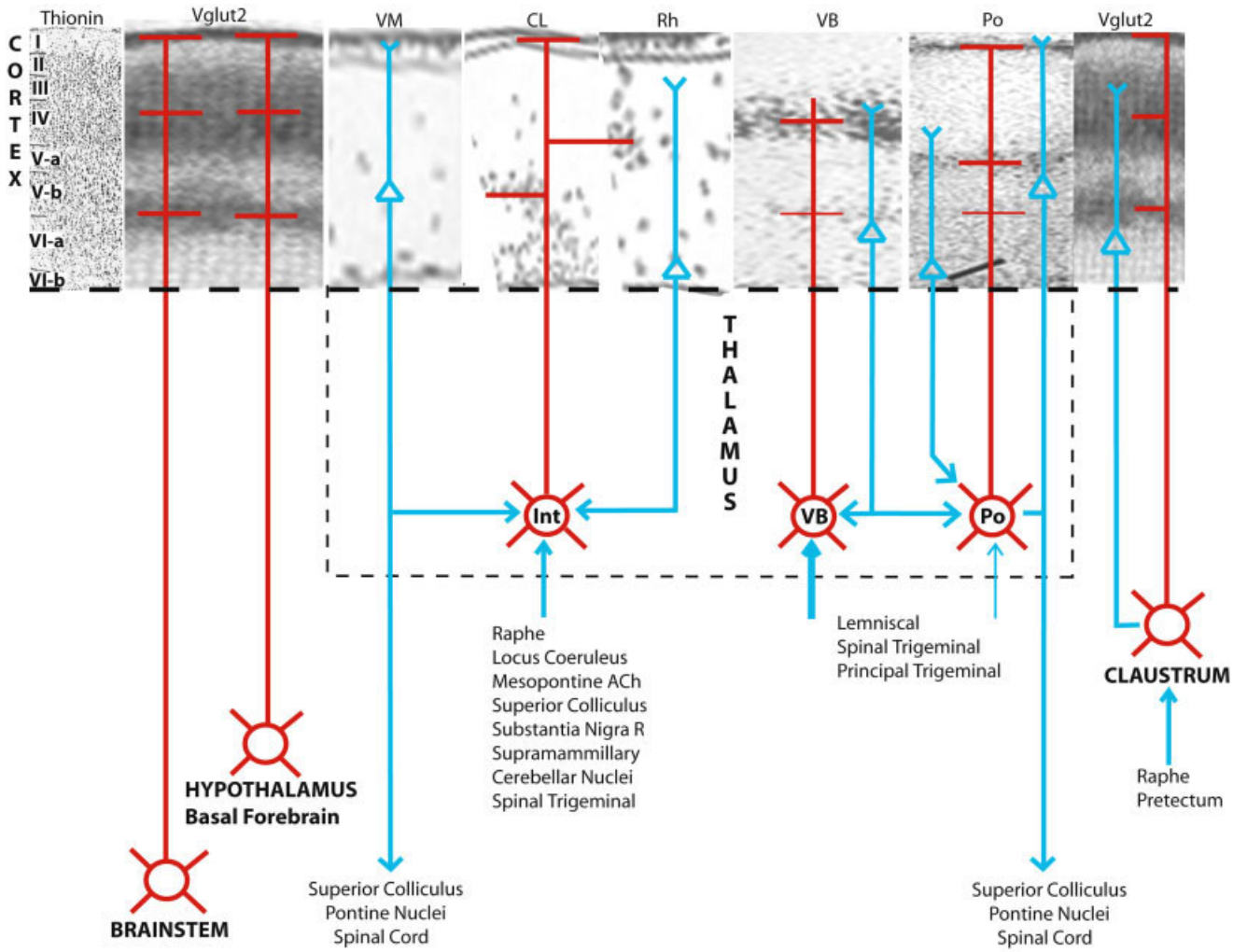

Fig. 12. A simplified diagram illustrating the main excitatory inputs to the somatosensory cortex. Blocks of cortical tissue were scaled to proportional size and represent the same cortical slab stained by various methods including thionin (Roman numeral indicate cortical layers; Krieg, 1946) and Vglut2 (Kaneko et al., 2002). Thalamic afferents are shown for the ventromedial (VM; Herkenham, 1979); centrolateral (CL; Berendse and Groenewegen, 1991); rhomboid (Rh; Van der Werf et al., 2002); ventrobasal nuclei (ventroposterior, VB, Herkenham, 1980); and the posterior complex (Po, Herkenham, 1980). Various ascending Vglut2 axons and their cortical arborizations are drawn in red; pyramidal neurons and their axonal outflow in blue. Some of the inputs to the thalamic nuclei, including intralaminar-midline (Int), VB, and Po are indicated. The major Vglut2 extrathalamic input originates in the hypothalamus, basal forebrain, brainstem, and the claustrum. The inputs to the thalamus and intracortical arborization of Vglut2 axons are weighted. Note that all of these pyramidal cells and subcortical inputs are superimposed in the same space of cortical tissue. Also note the thalamocortical axons arborize in Layer VI where Vglut2 terminals are not apparent. Oblique black line in the Po strip indicates scale bar (0.5 mm) according to Herkenham (1980).

to facilitate cortical plasticity (Tremblay et al., 1990; Aoki and Kabak, 1992; Mrzljak et al., 1993).

Amygdalocortical projection. The existence of amygdalocortical projections is well established in different species. In rodents, corticopetal projections originate in the lateral, basolateral, and basomedial nuclei (Pitkänen, 2000). From our study, the basolateral amygdaloid nucleus was heavily populated by single retrogradely labeled neurons following injection of the prefrontal or somatosensory cortex. In addition, cells in the basomedial, lateral, and anterior cortical nuclei projected to the prefrontal cortex. Less than 1% of the total corticopetal Vglut2 projection originates in the amygdaloid nuclei and this corresponds to 5% of the extrathalamic Vglut2 projection.

Claustrum. Of the extrathalamic Vglut2 projection, the claustrum provided 69% to the primary somatosensory and 42% to the mPFC. Thus, in addition to the hypothalamus, the claustral component is one of the two largest Vglut2 sources innervating the neocortex. The claustrum innervates the entire neocortex in a topographical manner in various species, including rats (Sarter and Markowisch, 1984; Sloniewski et al., 1986; Saper, 1987; Conde et al., 1995). Although the precise role of the claustrocortical projection is unclear, several groups suggested a role in modulating cortical receptive field properties (Sherk and LeVay, 1981; Tsumoto and Suda, 1982; Saper, 1987) or epileptogenesis (Sheerin et al., 2004). The widespread claustrocortical projection and the return Layer VI input to the claustrum (LeVay and Sherk, 1981) suggests

a role in cortical modulation similar to that of the thalamic intralaminar-midline nuclei.

Functional considerations

Vglut2-containing terminals show a trilaminar distribution in the cortex, specifically the upper part of Layer I, Layers II–IV, and the border between Layers Vb/VIa (Kaneko et al., 2002). In the somatosensory cortex, the terminal distribution of Vglut2 and those of various thalamocortical axons originating in thalamic nuclei that contain double-labeled cells in our study are shown in Figure 12 (Herkenham, 1986; Krettek and Price, 1977; Berendse and Groenewegen, 1991; Van der Werf et al., 2002). From this comparison, it is apparent that a single cortical area is likely to be innervated by Vglut2 axons from different thalamic nuclei that may terminate in different layers. Since various subtype-specific glutamate receptors show a complicated pattern in the neocortex, no clear-cut correlation can be established between Vglut2 terminals and specific glutamatergic receptor distribution (Shigemoto et al., 1992; Ohishi et al., 1993a,b; Conti et al., 1994a,b; Romano et al., 1995; Kinoshita et al., 1998; Petralia and Weinthold; 1992; Aoki et al., 1994; Valtschanoff et al., 1999).

Input to Layer IV in specific sensory cortical areas may subserve high-fidelity information transfer from the periphery (Steriade et al., 1997). Thalamocortical Layer I axons terminating on Layer I dendritic tufts of Layer V pyramidal neurons have been suggested to change the excitability of the main output neurons of the neocortex (Larkum et al., 1999; Zhu and Zhu, 2004). The concurrent arrival of Layer I and Layer IV inputs along the dendrites of Layer V pyramidal neurons promotes burst firing and nonlinear amplification of synaptic responses (Llinas et al., 2002; Zhu and Zhu, 2004). Thalamocortical cells from the midline-intralaminar nuclei terminate in Layer I. Assuming that the cortically projecting extrathalamic Vglut2 cells also terminate in Layer I, this extrathalamic Vglut2 projection may have a similar role in amplifying specific sensory information. Thus, the widespread projections from the extrathalamic Vglut2 cells to the neocortex may participate in diffuse activation of the neocortex.

It is interesting to note that many of the Vglut2-positive neurons projecting to the prefrontal or somatosensory cortices are located in the posterior lateral hypothalamic area (Figs. 5D, 6B, 10D), a site whose L-glutamate stimulation produced cardiovascular effects (Spencer et al., 1989; Gelsema et al., 1989). This region has been shown to be connected to cortical, brainstem, and spinal cord regions involved in sympathetic or parasympathetic regulation (Sun and Guyenet, 1986; Allen and Cechetto, 1992, 1993), suggesting that these neurons may be important in the integration of autonomic mechanisms with ascending arousal responses (Saper, 1995).

ACKNOWLEDGMENTS

We thank Drs. Patrice Guyenet and Ruth L. Stornetta, supported by NHLBI grants HL28785 and HL60003, for training and consultation during development of the in situ hybridization protocol.

LITERATURE CITED

Aihara Y, Mashima H, Onda H, Hisano S, Kasuya H, Hori T, Yamada S, Tomura H, Yamada Y, Inoue I, Kojima I, Takeda J. 2000. Molecular cloning of a novel brain-type Na(+)-dependent inorganic phosphate cotransporter. J Neurochem 74:2622–2625.

Akiyama H, Kaneko T, Mizuno N, McGeer PL. 1990. Distribution of phosphate-activated glutaminase in the human cerebral cortex. J Comp Neurol 297:239–252.

Allen GV, Cechetto DF. 1992. Functional and anatomical organization of cardiovascular pressor and depressor sites in the lateral hypothalamic area. I. Descending projections. J Comp Neurol 315:313–332.

Allen GV, Cechetto DF. 1993. Functional and anatomical organization of cardiovascular pressor and depressor sites in the lateral hypothalamic area. II. Ascending projections. J Comp Neurol 330:421–438.

Aoki C, Kabak S. 1992. Cholinergic terminals in the cat visual cortex: ultrastructural basis for interaction with glutamate-immunoreactive neurons and other cells. Vis Neurosci 8:177–191.

Aoki C, Venkatesan C, Go CG, Mong JA, Dawson TM. 1994. Cellular and subcellular localization of NMDA-R1 subunit immunoreactivity in the visual cortex of adult and neonatal rats. J Neurosci 14:5202–5222.

Aston-Jones G, Shipley MT, Grzanna R. 1995. The locus coeruleus, A5 and A7 noradrenergic cell groups. In: Paxinos G, editor. The rat nervous system. San Diego: Academic Press. p 183–213.

Bai L, Xu H, Collins JF, Ghishan FK. 2001. Molecular and functional analysis of a novel neuronal vesicular glutamate transporter. J Biol Chem 276:36764–36769.

Bellocchio EE, Hu H, Pohorille A, Chan J, Pickel VM, Edwards RH. 1998. The localization of the brain-specific inorganic phosphate transporter suggests a specific presynaptic role in glutamatergic transmission. J Neurosci 18:8648–8659.

Bellocchio EE, Reimer RJ, Fremeau RT Jr, Edwards RH. 2000. Uptake of glutamate into synaptic vesicles by an inorganic phosphate transporter. Science 289:957–960.

Berendse HW, Groenewegen HJ. 1991. Restricted cortical termination fields of the midline and intralaminar thalamic nuclei in the rat. Neuroscience 42:73–102.

Broberger C, De Lecea L, Sutcliffe JG, Hokfelt T. 1998. Hypocretin/orexin- and melanin-concentrating hormone-expressing cells form distinct populations in the rodent lateral hypothalamus: relationship to the neuropeptide Y and agouti gene-related protein systems. J Comp Neurol 402:460–474.

Buzsaki G, Bickford RG, Armstrong DM, Ponomareff G, Chen KS, Ruiz R, Thal LJ, Gage FH. 1988. Electric activity in the neocortex of freely moving young and aged rats. Neuroscience 26:735–744.

Clements JR, Grant S. 1990. Glutamate-like immunoreactivity in neurons of the laterodorsal tegmental and pedunculopontine nuclei in the rat. Neurosci Lett 120:70–73.

Conde F, Maire-Lepoivre E, Audinat E, Crepel F. 1995. Afferent connections of the medial frontal cortex of the rat. II. Cortical and subcortical afferents. J Comp Neurol 352:567–593.

Conti F, Minelli A, Molnar M, Brecha NC. 1994a. Cellular localization and laminar distribution of NMDAR1 mRNA in the rat cerebral cortex. J Comp Neurol 343:554–565.

Conti F, Minelli A, Brecha NC. 1994b. Cellular localization and laminar distribution of AMPA glutamate receptor subunits mRNAs and proteins in the rat cerebral cortex. J Comp Neurol 350:241–259.

Dahlström A, Fuxe K. 1964. Evidence for the existence of monoamine-containing neurons in the central nervous system. I. Demonstration of monoamines in the cell bodies if brainstem neurons. Acta Physiol Scand 232(Suppl 62):1–55.

Dal Bo G, St-Gelais F, Danik M, Williams S, Cotton M, Trudeau LE. 2004. Dopamine neurons in culture express VGLUT2 explaining their capacity to release glutamate at synapses in addition to dopamine. J Neurochem 88:1398–1405.

Detari L, Vanderwolf CH. 1987. Activity of identified cortically projecting and other basal forebrain neurones during large slow waves and cortical activation in anaesthetized rats. Brain Res 437:1–8.

Docherty M, Bradford HF, Wu JY. 1997. Co-release of glutamate and aspartate from cholinergic and GABAergic synaptosomes. Nature 330: 64–66.

Donoghue JP, Parham C. 1983. Afferent connections of the lateral agranular field of the rat motor cortex. J Comp Neurol 217:390–404.

Donoghue JP, Kerman KL, Ebner FF. 1979. Evidence for two organizational plans within the somatic sensory-motor cortex of the rat. J Comp Neurol 183:647–663.

Duque A, Balatoni B, Detari L, Zaborszky L. 2000. EEG correlation of the discharge properties of identified neurons in the basal forebrain. J Neurophysiol 84:1627–1635.

Fabri M, Burton H. 1991. Topography of connections between primary somatosensory cortex and posterior complex in rat: a multiple fluorescent tracer study. Brain Res 538:351–357.

Fallon JH, Loughlin SE. 1995. Substantia nigra. In: Paxinos G, editor. The rat nervous system. San Diego: Academic Press. p 215–237.

Faull RL, Carman JB. 1978. The cerebellofugal projections in the brachium conjunctivum of the rat. J Comp Neurol 178:495–518.

Forloni G, Grzanna R, Blakely RD, Coyle JT. 1987. Co-localization of N-acetyl-aspartyl-glutamate in central cholinergic, noradrenergic, and serotonergic neurons. Synapse 1:455–460.

Fremeau RT Jr, Troyer MD, Pahner I, Nygaard GO, Tran CH, Reimer RJ, Bellocchio EE, Fortin D, Storm-Mathisen J, Edwards RH. 2001. The expression of vesicular glutamate transporters defines two classes of excitatory synapse. Neuron 31:247–260.

Fremeau RT Jr, Burman J, Qureshi T, Tran CH, Proctor J, Johnson J, Zhang H, Sulzer D, Copenhagen DR, Storm-Mathisen J, Reimer RJ, Chaudhry FA, Edwards RH. 2002. The identification of vesicular glutamate transporter 3 suggests novel modes of signaling by glutamate. Proc Natl Acad Sci U S A 22:14488–14493.

Fremeau RT, Kam K, Qureshi T, Johnson J, Copenhagen DR, Storm-Mathisen J, Chaudhry FA, Nicoll RA, Edwards RH. 2004. Vesicular glutamate transporters 1 and 2 target to functionally distinct synaptic release sites. Science 304:1815–1819.

Fujiyama F, Furuta T, Kaneko T. 2001. Immunocytochemical localization of candidates for vesicular glutamate transporters in the rat cerebral cortex. J Comp Neurol 435:379–387.

Gras C, Herzog E, Bellenchi GC, Bernard V, Ravassard P, Pohl M, Gasnier B, Giros B, El Mestikawy S. 2002. A third vesicular glutamate transporter expressed by cholinergic and serotoninergic neurons. J Neurosci 22:5442–5451.

Gelsema AJ, Roe MJ, Calaresu FR. 1989. Neurally mediated cardiovascular responses to stimulation of cell bodies in the hypothalamus of the rat. Brain Res 482:67–77.

Gritti I, Mainville L, Mancia M, Jones BE. 1997. GABAergic and other noncholinergic basal forebrain neurons, together with cholinergic neurons, project to the mesocortex and isocortex in the rat. J Comp Neurol 383:163–177.

Groenewegen HJ. 1988. Organization of the afferent connections of the mediodorsal thalamic nucleus in the rat, related to the mediodorsal-prefrontal topography. Neuroscience 24:379–431.

Groenewegen HJ, Berendse HW. 1994. The specificity of the 'nonspecific' midline and intralaminar thalamic nuclei. Trends Neurosci 17:52–57.

Hajszan T, Alreja M, Leranth C. 2004. Intrinsic vesicular glutamate transporter 2-immunoreactive input to septohippocampal parvalbumin-containing neurons: novel glutamatergic local circuit cells. Hippocampus 14:499–509.

Harkany T, Holmgren C, Hartig W, Qureshi T, Chaudhry FA, Storm-Mathisen J, Dobszay MB, Berghuis P, Schulte G, Sousa KM, Fremeau RT Jr, Edwards RH, Mackie K, Ernfors P, Zilberter Y. 2004. Endocannabinoid-independent retrograde signaling at inhibitory synapses in layer 2/3 of neocortex: involvement of vesicular glutamate transporter 3. J Neurosci 24:4978–4988.

Herkenham M. 1979. The afferent and efferent connections of the ventromedial thalamic nucleus in the rat. J Comp Neurol 183:487–517.

Herkenham M. 1980. Laminar organization of thalamic projections to the rat neocortex. Science 207:532–535.

Herkenham M. 1986. New perspectives on the organization and evolution of nonspecific thalamocortical projections. In: Jones EG, Peters A, editors. Cerebral cortex, vol. 5. New York: Plenum Press. p 403–445.

Herzog E, Bellenchi GC, Gras C, Bernard V, Ravassard P, Bedet C, Gasnier B, Giros B, El Mestikawy S. 2001. The existence of a second vesicular glutamate transporter specifies subpopulations of glutamatergic neurons. J Neurosci 21:RC181.

Herzog E, Gilchrist J, Gras C, Muzerelle A, Ravassard P, Giros B, Gaspar P, El Mestikawy S. 2004. Localization of VGLUT3, the vesicular glutamate transporter type 3, in the rat brain. Neuroscience 123:983–1002.

Hioki H, Fujiyama F, Taki K, Tomioka R, Furuta T, Tamamaki N, Kaneko T. 2003. Differential distribution of vesicular glutamate transporters in the rat cerebellar cortex. Neuroscience 117:1–6.

Hisano S, Hoshi K, Ikeda Y, Maruyama D, Kanemoto M, Ichijo H, Kojima I, Takeda J, Nogami H. 2000. Regional expression of a gene encoding a neuron-specific Na+-dependent inorganic phosphate cotransporter (DNPI) in the rat forebrain. Mol Brain Res 83:34–43.

Hisano S, Sawada K, Kawano M, Kanemoto M, Xiong G, Mogi K, Sakata-Haga H, Takeda J, Fukui Y, Nogami H. 2002. Expression of inorganic phosphate/vesicular glutamate transporters (BNPI/VGLUT1 and DNPI/VGLUT2) in the cerebellum and precerebellar nuclei of the rat. Mol Brain Res 107:23–31.

Hur EE, Stornetta RL, Guyenet PG, Zaborszky L. 2002. Distribution of glutamate neurons in the basal forebrain as revealed by the presence of vesicular glutamate transporter (VGLUT2). Soc Neurosci Abstr 28, 239.4.

Jimenez-Capdeville ME, Dykes RW, Myasnikov AA. 1997. Differential control of cortical activity by the basal forebrain in rats: a role for both cholinergic and inhibitory influences. J Comp Neurol 381:53–67.

Jones EG. 1998. Viewpoint: the core and matrix of thalamic organization. Neuroscience 85:331–345.

Jones EG. 2001. The thalamic matrix and thalamocortical synchrony. Trends Neurosci 24:595–601.

Jones EG, Leavitt RY. 1974. Retrograde axonal transport and the demonstration of non-specific projections to the cerebral cortex and striatum from thalamic intralaminar nuclei in the rat, cat and monkey. J Comp Neurol 154:349–377.

Kaneko T, Mizuno N. 1988. Immunohistochemical study of glutaminase-containing neurons in the cerebral cortex and thalamus of the rat. J Comp Neurol 267:590–602.

Kaneko T, Nakaya Y, Mizuno N. 1992. Paucity of glutaminase-immunoreactive nonpyramidal neurons in the rat cerebral cortex. J Comp Neurol 322:181–190.

Kaneko T, Fujiyama F, Hioki H. 2002. Immunohistochemical localization of candidates for vesicular glutamate transporters in the rat brain. J Comp Neurol 444:39–62.

Kievit J, Kuypers HG. 1977. Organization of the thalamo-cortical connexions to the frontal lobe in the rhesus monkey. Exp Brain Res 29:299–322.

Kinoshita A, Shigemoto R, Ohishi H, Van der Putten H, Mizuno N. 1998. Immunohistochemical localization of metabotropic glutamate receptors, mGluR7a and mGluR7b, in the central nervous system of the adult rat and mouse: a light and electron microscopic study. J Comp Neurol 393:332–352.

Kosofsky BE, Molliver ME. 1987. The serotoninergic innervation of cerebral cortex: different classes of axon terminals arise from dorsal and median raphe nuclei. Synapse 1:153–168.

Krettek JE, Price JL. 1977. The cortical projections of the mediodorsal nucleus and adjacent thalamic nuclei in the rat. J Comp Neurol 171: 157–191.

Krieg WJS. 1946. Connections of the cerebral cortex. I. The albino rat.B. Structure of the cortical areas. J Comp Neurol 84:277–323.

Laake JH, Takumi Y, Eidet J, Torgner IA, Roberg B, Kvamme E, Ottersen OP. 1999. Postembedding immunogold labelling reveals subcellular localization and pathway-specific enrichment of phosphate activated glutaminase in rat cerebellum. Neuroscience 88:1137–1151.

Larkum ME, Zhu JJ, Sakmann B. 1999. A new cellular mechanism for coupling inputs arriving at different cortical layers. Nature 398:338–341.

Lavoie B, Parent A. 1994. Pedunculopontine nucleus in the squirrel monkey: cholinergic and glutamatergic projections to the substantia nigra. J Comp Neurol 344:232–241.

LeVay S, Sherk H. 1981. The visual claustrum of the cat. I. Structure and connections. J Neurosci 1:956–980.

Li JL, Xiong KH, Dong YL, Fujiyama F, Kaneko T, Mizuno N. 2003. Vesicular glutamate transporters, VGluT1 and VGluT2, in the trigeminal ganglion neurons of the rat, with special reference to coexpression. J Comp Neurol 463:212–220.

Lin W, McKinney K, Liu L, Lakhlani S, Jennes L. 2003. Distribution of vesicular glutamate transporter-2 messenger ribonucleic acid and protein in the septum-hypothalamus of the rat. Endocrinology 144:662–670.

Llinas RR, Leznik E, Urbano FJ. 2002. Temporal binding via cortical coincidence detection of specific and nonspecific thalamocortical inputs: a voltage-dependent dye-imaging study in mouse brain slices. Proc Natl Acad Sci U S A 99:449–454.

Lorente de No R. 1938. Cerebral cortex: architecture, intracortical connections, motor projections. In: Fulton J, editor. Physiology of the nervous system. London: Oxford University Press. p 291–340.

Manns ID, Alonso A, Jones BE. 2000. Discharge properties of juxtacellularly labeled and immunohistochemically identified cholinergic basal forebrain neurons recorded in association with the electroencephalogram in anesthetized rats. J Neurosci 20:1505–1518.

Manns ID, Mainville L, Jones BE. 2001. Evidence for glutamate, in addition to acetylcholine and GABA, neurotransmitter synthesis in basal

forebrain neurons projecting to the entorhinal cortex. Neuroscience 107:249–263.

Marcus JN, Aschkenasi CJ, Lee CE, Chemelli RM, Saper CB, Yanagisawa M, Elmquist JK. 2001. Differential expression of orexin receptors 1 and 2 in the rat brain. J Comp Neurol 435:6–25.

Mrzljak L, Levey AI, Goldman-Rakic PS. 1993. Association of m1 and m2 muscarinic receptor proteins with asymmetric synapses in the primate cerebral cortex: morphological evidence for cholinergic modulation of excitatory neurotransmission. Proc Natl Acad Sci U S A 90:5194–5198.

Ni B, Rosteck PR Jr, Nadi NS, Paul SM. 1994. Cloning and expression of a cDNA encoding a brain-specific Na+-dependent inorganic phosphate cotransporter. Proc Natl Acad Sci U S A 91:5607–5611.

Ohishi H, Shigemoto R, Nakanishi S, Mizuno N. 1993a. Distribution of the messenger RNA for a metabotropic glutamate receptor, mGluR2, in the central nervous system of the rat. Neuroscience 53:1009–1018.

Ohishi H, Shigemoto R, Nakanishi S, Mizuno N. 1993b. Distribution of the mRNA for a metabotropic glutamate receptor (mGluR3) in the rat brain: an in situ hybridization study. J Comp Neurol 335:252–266.

Paxinos G, Watson C. 1998. The rat brain in stereotaxic coordinates. San Diego: Academic Press.

Petralia RS, Wenthold RJ. 1992. Light and electron immunocytochemical localization of AMPA-selective glutamate receptors in the rat brain. J Comp Neurol 318:329–354.

Peyron C, Tighe DK, Van den Pol AN, de Lecea L, Heller HC, Sutcliffe JG, Kilduff TS. 1998. Neurons containing hypocretin (orexin) project to multiple neuronal systems. J Neurosci 18:9996–10015.

Pitkänen A. 2000. Connectivity of the rat amygdaloid complex. In: Aggleton JP, editor. The amygdala: a functional analysis, 2nd ed. Oxford: Oxford University Press. p 31–115.

Price JL. 1995. Thalamus. In: Paxinos G, editor. The rat nervous system. San Diego: Academic Press.

Reep RL, Corwin JV. 1999. Topographic organization of the striatal and thalamic connections of rat medial agranular cortex. Brain Res 841:43–52.

Reep RL, Chandler HC, King V, Corwin JV. 1994. Rat posterior parietal cortex: topography of corticocortical and thalamic connections. Exp Brain Res 100:67–84.

Reep RL, Corwin JV, King V. 1996. Neuronal connections of orbital cortex in rats: topography of cortical and thalamic afferents. Exp Brain Res 111:215–232.

Romano C, Sesma MA, McDonald CT, O'Malley K, Van den Pol AN, Olney JW. 1995. Distribution of metabotropic glutamate receptor mGluR5 immunoreactivity in rat brain. J Comp Neurol 355:455–469.

Rosin DL, Weston MC, Sevigny CP, Stornetta RL, Guyenet PG. 2003. Hypothalamic orexin (hypocretin) neurons express vesicular glutamate transporters VGLUT1 or VGLUT2. J Comp Neurol 465:593–603.

Sanderson KJ, Dreher B, Gayer N. 1991. Prosencephalic connections of striate and extrastriate areas of rat visual cortex. Exp Brain Res 85:324–334.

Saper CB. 1984. Organization of cerebral cortical afferent systems in the rat. II. Magnocellular basal nucleus. J Comp Neurol 222:313–342.

Saper CB. 1985. Organization of cerebral cortical afferent systems in the rat. II. Hypothalamocortical projections. J Comp Neurol 237:21–46.

Saper CB. 1987. Diffuse cortical projection systems: anatomical organization and role in cortical function. In: Handbook of physiology, sect. 1. The nervous system, vol. 5. Part 1. Bethesda, MD: Am Physiol Soc 169–209.

Saper CB. 1995. Central autonomic system. In: Paxinos G, editor. The rat nervous system. San Diego: Academic Press. p 107–135.

Sarter M, Markowitsch HJ. 1984. Collateral innervation of the medial and lateral prefrontal cortex by amygdaloid, thalamic, and brain-stem neurons. J Comp Neurol 224:445–460.

Satoh K, Fibiger HC. 1986. Cholinergic neurons of the laterodorsal tegmental nucleus: efferent and afferent connections. J Comp Neurol 253:277–302.

Schafer MK, Varoqui H, Defamie N, Weihe E, Erickson JD. 2002. Molecular cloning and functional identification of mouse vesicular glutamate transporter 3 and its expression in subsets of novel excitatory neurons. J Biol Chem 52:50734–50748.

Sheerin AH, Nylen K, Zhang X, Saucier DM, Corcoran ME. 2004. Further evidence for a role of the anterior claustrum in epileptogenesis. Neuroscience 125:57–62.

Sherk H, LeVay S. 1981. The visual claustrum of the cat. III. Receptive field properties. J Neurosci 1:993–1002.

Shigemoto R, Nakanishi S, Mizuno N. 1992. Distribution of the mRNA for a metabotropic glutamate receptor (mGluR1) in the central nervous system: an in situ hybridization study in adult and developing rat. J Comp Neurol 322:121–135.

Shipley MT, McLean JH, Ennis M. 1995. Olfactory system. In: Paxinos G, editor. The rat nervous system, 2nd ed. San Diego: Academic Press. p 899–926.

Sloniewski P, Usunoff KG, Pilgrim C. 1986. Retrograde transport of fluorescent tracers reveals extensive ipsi- and contralateral claustrocortical connections in the rat. J Comp Neurol 246:467–477.

Somogyi J, Baude A, Omori Y, Shimizu H, Mestikawy SE, Fukaya M, Shigemoto R, Watanabe M, Somogyi P. 2004. GABAergic basket cells expressing cholecystokinin contain vesicular glutamate transporter type 3 (VGLUT3) in their synaptic terminals in hippocampus and isocortex of the rat. Eur J Neurosci 19:552–569.

Spencer SE, Sawyer WB, Loewy AD. 1989. Cardiovascular effects produced by L-glutamate stimulation of the lateral hypothalamic area. Am J Physiol 257:H540–552.

Steriade M, Jones EG, McCormick DA. 1997. Thalamus, vol. 1. Organisation and function. Oxford: Elsevier Science.

Stornetta RL, Sevigny CP, Guyenet PG. 2002. Vesicular glutamate transporter DNPI/VGLUT2 mRNA is present in C1 and several other groups of brainstem catecholaminergic neurons. J Comp Neurol 444:191–206.

Sun MK, Guyenet PG. 1986. Hypothalamic glutamatergic input to medullary sympathoexcitatory neurons in rats. Am J Physiol 251:R798–810.

Szerb JC, Fine A. 1990. Is glutamate a co-transmitter in cortical cholinergic terminals? Effects of nucleus basalis lesion and of presynaptic muscarinic agents. Brain Res 515:214–218.

Takamori S, Rhee JS, Rosenmund C, Jahn R. 2000. Identification of a vesicular glutamate transporter that defines a glutamatergic phenotype in neurons. Nature 407:189–194.

Takamori S, Malherbe P, Broger C, Jahn R. 2002. Molecular cloning and functional characterization of human vesicular glutamate transporter 3. EMBO Rep 3:798–803.

Takeda N, Inagaki S, Taguchi Y, Tohyama M, Watanabe T, Wada H. 1984. Origins of histamine-containing fibers in the cerebral cortex of rats studied by immunohistochemistry with histidine decarboxylase as a marker and transection. Brain Res 323:55–63.

Thompson SM, Robertson RT. 1987. Organization of subcortical pathways for sensory projections to the limbic cortex. I. Subcortical projections to the medial limbic cortex in the rat. J Comp Neurol 265:175–188.

Tremblay N, Warren RA, Dykes RW. 1990. Electrophysiological studies of acetylcholine and the role of the basal forebrain in the somatosensory cortex of the cat. I. Cortical neurons excited by glutamate. J Neurophysiol 64:1199–1211.

Tsumoto T, Suda K. 1982. Effects of stimulation of the dorsocaudal claustrum on activities of striate cortex neurons in the cat. Brain Res 240:345–349.

Valtschanoff JG, Burette A, Wenthold RJ, Weinberg RJ. 1999. Expression of NR2 receptor subunit in rat somatic sensory cortex: synaptic distribution and colocalization with NR1 and PSD-95. J Comp Neurol 410:599–611.

Van der Werf YD, Witter MP, Groenewegen HJ. 2002. The intralaminar and midline nuclei of the thalamus. Anatomical and functional evidence for participation in processes of arousal and awareness. Brain Res Brain Res Rev 39:107–140.

Van Groen T, Wyss JM. 1992. Projections from the laterodorsal nucleus of the thalamus to the limbic and visual cortices in the rat. J Comp Neurol 324:427–448.

Wojcik SM, Rhee JS, Herzog E, Sigler A, Jahn R, Takamori S, Brose N, Rosenmund C. 2004. An essential role for vesicular glutamate transporter 1 (VGLUT1) in postnatal development and control of quantal size. Proc Natl Acad Sci U S A 101:7158–7163.

Zaborszky L, Duque A. 2003. Sleep-wake mechanisms and basal forebrain circuitry. Front Biosci 8:d1146–1169.

Zaborszky L, Carlsen J, Brashear HR, Heimer L. 1986. Cholinergic and GABAergic afferents to the olfactory bulb in the rat with special emphasis on the projection neurons in the nucleus of the horizontal limb of the diagonal band. J Comp Neurol 243:488–509.

Zaborszky L, Pang K, Somogyi J, Nadasdy Z, Kallo I. 1999. The basal forebrain corticopetal system revisited. Ann N Y Acad Sci 877:339–367.

Zhu Y, Zhu JJ. 2004. Rapid arrival and integration of ascending sensory information in layer 1 nonpyramidal neurons and tuft dendrites of layer 5 pyramidal neurons of the neocortex. J Neurosci 24:1272–2179.

Ziegler DR, Cullinan WE, Herman JP. 2002. Distribution of vesicular glutamate transporter mRNA in rat hypothalamus. J Comp Neurol 448:217–229.